Interaction of Chemical Contaminants with Suspended Particles and Attached Inorganic Deposits in Drinking Water Systems

Dina Alexandra Oliveira Martins

Dissertation presented to obtain the degree of
DOCTOR IN ENVIORMENTAL ENGINEERING
by the University of Porto

Doctor Luís Manuel Ferreira Melo
(Supervisor)

Doctor Manuel José Vieira Simões
(co-supervisor)

Porto, 2014

“On the mountains of truth you can never climb in vain:

either you will reach a point higher up today,

or you will be training your powers so that

you will be able to climb higher tomorrow."

Friedrich Nietzsche

Acknowledgments

First of all, I would like to express my gratitude for my PhD grant and the opportunity to be a part of the European Research Project SecurEau (http://www.secureau.eu/ – Contract no. 217976), supported by the European Commission within the 7th Framework Programme FP7-SEC-2007-1 – "Security; Increasing the security of Citizen; Water distribution surveillance"

I would also like to express my gratitude to FEUP (Faculty of Engineering of the University of Porto), to DCE (Department of Chemical Engineering) and to LEPABE (Laboratory for Process Engineering, Environment, Biotechnology and Energy) for allowing me to access of their facilities and resources, making it possible to conduct my research work.

Foremost I would like to express my special thanks to my supervisor Professor Luis Melo and co-supervisor Professor Manuel Simões for their continuous guidance, support, patience and encouragement throughout my studies. It has been a privilege to have the opportunity to work and learn from you.

I would also like to thank Professors Arminda Alves, Margarida Bastos, Fernando Pereira and Eng. Luis Matos for the given support regarding analytical techniques and equipments.

To all my colleagues from E007 and project co-workers (Cátia and Raquel), especially to Mónica, for all the support, patience and encouragement I thank you all.

My special thanks to my friend Carla, for her patience, guidance and for always being there when I needed.

To all of those, within the Chemical Engineering Department, administrative and technical staff members, that I did not personally mention but that assisted me in my work every time I needed, I would like to leave a word of affection and gratitude for their availability and kindness.

Finally I would like to show my gratitude to João, my family and my close friends, for their unconditional love, tolerance and endless moral support and for always believing in me.

Without all of you I would not be where I am.

This thesis is dedicated to João and my family.

Abstract

Drinking water distribution systems accumulate several particulate matter in the form of suspended particles or adhered deposits that buildup in pipes and reservoirs, due to water flow. The particulate matter can have different sources (inorganic, organic or biological) resulting in deposits with a complex and miscellaneous composition. This makes the study of interaction of real deposits with chemical contaminants difficult, due to the wide range of possible outcomes. Clays and metal oxides are the most abundant inorganic minerals in natural systems. Thus, to overcome the complexity of real deposits composition, these two groups of substances were selected in order to initiate the gradual process of understanding the cause-effect associations between the components of the deposits found in the drinking water systems and pesticides that may be used to contaminate drinking water infrastructures.

In order to evaluate the possible outcomes of a contamination of drinking water networks by pesticides, some chemicals were selected and its sorption onto inorganic particle suspensions and sediments (attached deposits) was studied, considering several environmental conditions.

The chemicals selected for this study were paraquat dichloride (herbicide), chlorfenvinphos (insecticide) and carbofuran (insecticide). These chemicals are extremely toxic and its misuse can seriously affect public health.

This work intended to study the sorption phenomena of the selected pesticides onto inorganic particles (kaolin and hematite) and sediments,

evaluate the parameters that would influence the adsorption process and determine the adsorption kinetic parameters.

Paraquat was studied in both suspended particles and attached deposits in order to determine kinetic parameters and compare these two possibilities. Preliminary studies performed with chlorfenvinphos and carbofuran were only performed with suspended particles.

Under the studied conditions, the adsorption experiments performed with suspended kaolin particles led to removal percentages of 18, 16 and 22% for paraquat, carbofuran and chlorfenvinphos respectively. Mixed particle suspensions (kaolin plus iron (III) oxide)) applied in paraquat and carbofuran adsorption registered 18 and 24%, of chemical removal from the aqueous solution, respectively. With all pesticides, adsorption occurred very quickly, with an equilibrium plateau being reached in general after five minutes of interaction.

With paraquat, the effect of several process parameters (initial pH, sorbent dosage and stirring speed) were investigated. Experimental data were adjusted using pseudo-first and pseudo-second order models and kinetic parameters were determined. Results show that both models describe quite well the adsorption process presenting correlation coefficients around 0.99.

Regarding the equilibrium data gathered from the experimental assays, these were best adjusted using the Langmuir isotherm which presents higher correlation coefficient values and smaller normalized standard deviations than the Freundlich isotherm.

Experiments performed with adhered deposits resulted in 19 and 72% of paraquat removal using kaolin and mixed deposits, respectively. In mixed deposits, iron (III) oxide appears to play an important role, enhancing the mass transfer area and consequently promoting an improvement in the adsorption capacity of these deposits.

The studies performed with chlorfenvinphos and carbofuran allowed the gathering of preliminary information important to better understand these chemicals when in contact with the selected sorbents.

Some parameters (initial pH, temperature and stirring speed) were investigated, regarding chlorfenvinphos adsorption process. Results showed that the adsorption process seems to be favored by higher values of temperature and hampered by basic pH values. Variations in the agitation speed did not seem to affect de adsorption process.

Regarding carbofuran adsorption, the initial pH was the only parameter studied. The obtained results showed that a higher pH promotes a more efficient adsorption of this pesticide. Within acid and neutral media the obtained results were identical, indicating that, within this range (pH 3 and 7), this parameter does not exert any influence on the adsorption process.

Resumo

Os sistemas de distribuição de água potável tendem a acumular partículas que se apresentam sob a forma de suspensões ou depósitos aderidos, que se desenvolvem em tubagens e reservatórios, devido ao escoamento de água. As partículas que circulam pela rede de água potável podem ter diferentes origens (inorgânica, orgânica ou biológica), resultando em depósitos com uma composição diversa e complexa. Isto faz com que o estudo da interação de depósitos reais com contaminantes químicos seja bastante difícil, devido à ampla gama de resultados possíveis. As argilas e óxidos de metal são os componentes inorgânicos mais abundantes em sistemas naturais. Deste modo, para ultrapassar as limitações associadas à complexidade dos depósitos reais, estes dois componentes foram selecionados, para dar início ao processo gradual de compreensão das relações causa-efeito entre os componentes dos depósitos encontrados na rede de água potável e pesticidas que podem ser utilizados para contaminar as várias infra-estruturas.

Por forma a avaliar os possíveis resultados de uma contaminação da rede de água potável com pesticidas, alguns químicos foram selecionados e sua eventual adsorção em partículas inorgânicas suspensas e sedimentos (depósitos aderidos) foi estudada, considerando diversas condições ambientais.

Os pesticidas selecionados para este estudo foram: paraquato (herbicida), clorfenvinfos (inseticida) e carbofurano (inseticida). Estes

pesticidas são extremamente tóxicos e a sua utilização imprópria pode afetar seriamente a saúde pública.

Este trabalho de investigação teve como objetivo o estudo dos fenómenos de adsorção entre os pesticidas selecionados e partículas inorgânicas (caulino e hematite) em suspensão ou sedimentos, a avaliação do efeito de diferentes parâmetros no processo de adsorção e a determinação de parâmetros cinéticos.

A adsorção de paraquat foi estudada quer em partículas suspensas, quer em depósitos aderidos de modo a determinar os parâmetros cinéticos e comparar estas duas possibilidades. Os estudos preliminares realizados com clorfenvinfos e carbofurano só foram realizados com partículas em suspensão.

Nas condições estudadas, os ensaios de adsorção realizados com partículas de caulino promoveram a remoção de 18, 16 e 22% de paraquato, carbofurano e clorfenvinfos, respetivamente. As suspensões mistas (caulino com hematite) aplicadas nos estudos de adsorção de paraquato e carbofurano registaram, respetivamente, 18 e 24% de remoção destes pesticidas da solução aquosa. Com todos os pesticidas estudados, a adsorção ocorreu muito rapidamente sendo alcançado o patamar de equilíbrio, em geral, após cinco minutos de interação.

O efeito de vários parâmetros (pH inicial, quantidade de adsorvente e velocidade de agitação) na adsorção de paraquato foi estudado e avaliado. Os dados experimentais foram ajustados usando modelos de pseudo-primeira e pseudo-segunda ordens e os parâmetros cinéticos

foram determinados. Os resultados indicam que ambos os modelos descrevem bem o processo de adsorção, apresentando coeficientes de correlação da ordem de 0,99.

Em relação aos dados recolhidos dos ensaios de equilíbrio, a isotérmica de Langmuir apresenta um melhor ajuste, exibindo valores de coeficientes de correlação superiores e desvios padrões normalizados inferiores comparativamente à isotérmica de Freundlich.

As experiências realizadas com os depósitos aderidos resultaram em 19 e 72% de remoção de paraquat utilizando depósitos de caulino e mistos, respetivamente. Em depósitos mistos, o óxido de ferro (III), parece desempenhar um papel importante, aumentando a área de transferência de massa e, por conseguinte, promovendo uma melhoria da capacidade de adsorção destes depósitos.

Os estudos realizados com clorfenvinfos e carbofurano possibilitaram a recolha de informação preliminar importante para uma melhor compreensão da adsorção destes químicos.

Alguns parâmetros (pH inicial, temperatura e velocidade de agitação) foram investigados de modo a aprofundar a compreensão do processo de adsorção do chlorfenvinphos. Os resultados obtidos indicam que o processo de adsorção parece ser favorecido por temperaturas elevadas e dificultado por valores de pH básicos. Por outro lado, a variação da velocidade de agitação não parece afetar o processo de adsorção deste químico.

Relativamente à adsorção de carbofurano, somente o efeito do pH foi investigado. Os resultados obtidos indicam que pHs básicos promovem o aumento de carbofurano adsorvido. Com valores de pH ácido e neutro, os resultados obtidos indicam que nesta gama (pH 3 e 7) este parâmetro não exerce influência no processo de adsorção.

Table of contents

Figure caption

Table caption

Nomenclature

Abbreviations

LNEG - Laboratório Nacional de Energia e Geologia

CEMUP - Centro de Materiais da Universidade do Porto

HPLC - High performance liquid chromatography

HFBA – Heptafluorobutyric Acid

SEM - Scanning electron microscopy

SD - Normalized standard deviation

AS - Agitation speed

$P_{K/IO}$ – Proportion between kaolin and iron (III) oxide quantities

Notation

A - Mass transfer area of the solid surface (m^2)

A_s - Sorbent area (m^2)

C_b - Concentration of solute in the bulk solution (kg m^{-3})

C_s - Concentration of solute at the interface (kg m^{-3})

C_e - Concentration of solute in solution at equilibrium (mg L^{-1})

C – Concentration of solute over time in the bulk solution (mg L^{-1})

C_0 - Initial concentration of solute in the bulk solution (mg L^{-1})

C_{PQ} - Paraquat concentration in the bulk solution (mg L^{-1})

d - Particle diameter (m)

D_v - Diffusivity of solute in the liquid (m^2 s^{-1})

g - Gravitational constant (m s^{-2})

Ga - Gallileo number

J - Mass transfer rate of solute (kg s^{-1})

k_1 - Rate constant of pseudo-first order sorption model (min^{-1})

k_2 - Rate constant of pseudo-second order sorption model (g mg^{-1} min^{-1})

K_L - Adsorption equilibrium constant of Langmuir isotherm (L mg^{-1})

K_F - Adsorption equilibrium constant of Freundlich isotherm (mg g^{-1}(mg L^{-1})$^{-1/n}$)

k_m – Individual mass transfer coefficient of the solute (m s^{-1})

k_{LS} – Global mass transfer coefficient in the liquid-solid interphase (m s^{-1})

M - Total mass of the solute remaining in the solid phase (kg)

n - Amount of data points

n_F - Freundlich isotherm constant

P - t-student test analysis parameter

q_e - Amount of solute adsorbed at equilibrium (mg g^{-1})

q_t - Amount of solute on the surface of the sorbent at any time (mg g^{-1})

q_{max} - Maximum adsorption capacity of the adsorbent (mg g^{-1})

R^2 - Correlation coefficient

Re - Reynolds number

Sh - Sherwood number

Sc - Schmidt number

t - Time (min)

T - Vessel diameter (m)

U – M $\rho^{-1}d^{-3}$, solid concentration

V_L - liquid volume (m^3)

Greek symbols

ρ - Density of liquid (kg m^{-3})

ω - Stirrer angular velocity (s^{-1})

ν - Kinematic viscosity of the liquid (m^2 s^{-1})

μ - Viscosity of the liquid (kg m^{-1} s^{-1})

Chapter 1.

Introduction

1.1. Drinking water systems and public health

In this century, one of the major problems that humanity faces concerns the quantity and/or quality of water.

Only 3% of the total water on Earth is fresh water and only 0.01% of it is available for human consumption. In the modern world this small portion of available water is continuously threatened by the requirements of a rapid growing population [1]. The lack of sanitation conditions and safe drinking water constitute the factors with harsher impact, affecting over a third of the world's population [2].

Availability of clean water is a basic need for human existence and the concept of public water supplies comes from ancient times [3]. To an ever growing civilization is essential to have a good infrastructure, able to distribute clean water of high and uniform quality and to provide the removal and treatment of effluents resulting from everyday activities in a modern society [4].

Among other factors, the importance of clean water led to a public health era in the mid-1850s [5] and a decade ago the General Assembly of the United Nations recognized that water is critical for a sustainable environmental development, human health and well-being. On the other hand it was detected that in developing countries, about half of the population live with insufficient water quality [6].

The entire infrastructure of drinking water and waste management is vital for sustaining society development, but it is also vulnerable to

intentional disruptions such as terrorist attacks. Water infrastructures such as dams, reservoirs or pipelines can be direct targets or they can be indirectly affected by the introduction of poisonous or disease-causing agents in the network [4].

Several chemical contaminants, with inorganic and organic origins, have been identified in drinking water [5]. These water pollutants can be sorted in two groups: macro-pollutants, a relatively small number of mostly inorganic pollutants occurring at levels of milligrams per liter, which sources and impacts are reasonably understood but sustainable technologies for treatment are still a research field; and micro-pollutants that consist of trace pollutants of organic and inorganic origins at the nanogram to microgram per liter levels. Several contaminants included in this second group can promote toxic effects at low concentrations, especially when they are a part of a chemical mixture [2].

The presence of pollutants in water can cause several different effects. A simple disagreable odor or taste is easily detected by the population and the process of characterization and identification of the causing pollutant is generally quick and straightforward. On the other hand, the presence in the water of a disease-causing agent, such as a carcinogenic compound, will probably go undetected, especially if it induces only a slight increase in the incidence of a common cancer [3].

Among the main sources of common water pollutants, many can be found in activities like mining, manufacturing, farming and runoffs from

urban and agricultural expansions [7]. Other possibility is a deliberate contamination of drinking water distribution networks.

1.2. Research motivation and scope

In the modern world one of the greater concerns is the risk that chemical weapons may be used by regular forces or by terrorist groups [8]

The studies compiled in this thesis were performed in the framework of the European project SECUREAU (7th Framework Program). The idea behind the project scope was the security and decontamination of drinking water distribution systems following a deliberate contamination and its main scientific goal was to launch an appropriate response for rapidly restoring the use of the drinking water network upon the occurrence of this situation (http://www.secureau.eu).

The studies here presented intended to provide kinetic parameters for the project's work package regarding the modeling of reactive transport in drinking water distribution systems in order to simulate the spread of contaminants throughout the network and the identification of the origin point(s) of the contamination.

In order to evaluate the possible outcomes of a contamination of drinking water networks using pesticides, some chemicals were selected and studied in terms of sorption kinetics onto inorganic particle

suspensions and sediments (attached deposits) and also their persistence under several different environmental conditions.

The chemicals selected for this study were paraquat dichloride (herbicide), chlorfenvinphos (insecticide) and carbofuran (insecticide).

Chlorfenvinphos and carbofuran, respectively belonging to organophosphate and carbamate groups, are highly toxic acetylcholinesterase inhibitors and can be used as neurotoxic agents also known as nerve agents, causing this way highly deleterious effects on humans. These chemicals are responsible for poisoning epidemics, especially in developing countries, such as Central American countries [9].

Paraquat is a quaternary ammonium herbicide, highly soluble in water (620 g L^{-1} at 20 ºC) [10]. This compound is extremely toxic, causing several health problems such as irreversible damage to the lungs, which are the primary target [11]. Since there is no antidote to reverse the effects of this chemical on the human body, the current use of paraquat results in a serious health risk [12].

Although restricted in developed countries, these chemicals are still used in underdeveloped countries, and therefore may be easily and uncontrollably sold, being by this way easily available for terrorist purposes.

Chapter 2.

Literature Review

2.1. Pesticide contaminants

This kind of chemicals stands out as one of the most important improvements to the efficiency of twentieth century agriculture. Over a decade ago, more than five hundred compounds were registered worldwide as pesticides or metabolites of pesticides [13]. Along the years, however, concerns regarding the effect of the extensive use of pesticides on mankind, flora and fauna, have been increasing. Even though pesticides offer irrefutable advantages, they are still poisons and can represent a great danger when misused [14].

The term pesticide stands for any chemical agent that is deliberately and legally used to prevent, destroy, repel or control any living species considered a pest [7]. Their patterns of application, interaction with the environment and unique chemical structure are what define pesticides. Their chemical structure allows them to mimic and consequently replace specific molecules in targeted biological reactions [15].

Pesticides can be categorized considering two main criteria: chemical classes based on the functional groups in their molecular structure (inorganic, organonitrogen, organohalogen, or organosulfur compounds) [13] or their target organism, based on their potential to kill living organisms (Table 1).

The most commonly applied pesticides are herbicides, followed by insecticides and fungicides [13].

Table 1: Pesticides' categorization according to their applications [7].

Pesticide category	Applications / Main target
Acaricides or miticides	Kill mice, tick and spiders that feed on plant and animals
Algicides	Kill algae in ponds, lakes, canals, swimming pools and industrial air-conditioners
Antifouling agents	Kill and/or prevent the attachment of organisms (such as barnacles) that attach to boat bottoms and other underwater surfaces
Avicides	Kill birds
Biocides	Kill microorganisms
Bio-pesticides	Pesticides obtained from natural materials.
Defoliants	Cause leaves or other foliage to die and drop from trees and plants
Disinfectants	Kill microorganisms on inanimate surfaces
Fumigants	Gases or fumes that kill insects, fungi and other unwanted species in building or soil.
Fungicide	Kill fungi, including blights, molds, mildews and rusts
Growth regulators	Disrupt life processes of insects or plants
Herbicides	Kill weeds (unwanted plants), grasses, and other plants.
Insecticides	Kill insects and arthropods
Molluscicides	Kill snails and slugs
Nematicides	Kill nematodes (microscopic, worm-like organisms that feed on plant roots)
Ovicides	Kill eggs of mites and insects
Piscicides	Kill fish
Predacides	Kill vertebrate predators
Repellants	Repel insects and birds
Rodenticides	Kill mice, rats and other rodents
Sanitizers	Kill microorganisms on skin (generally added to soaps and cleaners used in medical setting and at home)
Synergists	Enhance the killing power of active ingredients (nontoxic alone)

Pesticides can be found everywhere in the environment, contaminating virtually all sources of clean water [7] and this may lead to adverse effects to the public health and the environment (Table 2) [16].

Table 2: Most commonly used pesticides and associated health hazards [16].

Pesticides	Diseases / Adverse effects
Aldrin	Attack to the nervous system; convulsions; carcinogenic
Benzene hexachloride (BHC)	Liver tumor
Captan	Abnormality in eyes and brain; carcinogenic
Chlordane	Carcinogenic
Dichloro**d**iphenyl**t**richloroethane (DDT) and Haptachlor	Liver damage; carcinogenic
Dieldri	Liver damage; carcinogenic; destroys enzymatic activities
Endosulfan	Carcinogenic
Hexachlorocyclohexane (HCH)	Highly toxic; bone marrow damage; mutagenic; teratogenic; carcinogenic
Melathion, Methoxychlor	Low toxicity but sometimes carcinogenic

In addition to the information presented in Table 2, some other examples the effects of acute exposure to pesticide are neurobehavioral disorders, autoimmune diseases, reproductive abnormalities, deformities, life-threatening bleeding and myositis with burning sensation in the mouth and throat, nausea, vomiting, sweating, hyperventilation, etc. [15].

All people are inevitably exposed to pesticides by one of different routes such as inhalation, ingestion or dermal contact. Exposure may occur through environmental contamination or occupational use or in the case of general population through contact with pesticide residues, including physical and biological degradation of products in air, water and food [17].

Only a part of the applied amount of a pesticide is bioactive while the rest is distributed in the environment. The presence of these chemicals in water, soil, and air has raised concerns regarding environmental

protection, in particular the safety of drinking water quality [18], since pesticides have been detected in some water supplies as early as 1945 [19].

Developed countries have become very strict when it comes to water treatment, especially regarding pesticide compounds. Most of these chemicals have been considered priority substances in the Water Framework Directive established by the European Community in 2001 [20]. Within the European Union, pesticide analytical control is mandatory in different water bodies, including drinking, groundwater and surface waters [21].

The impact of pesticides in today's society is studied in several areas (Figure 1).

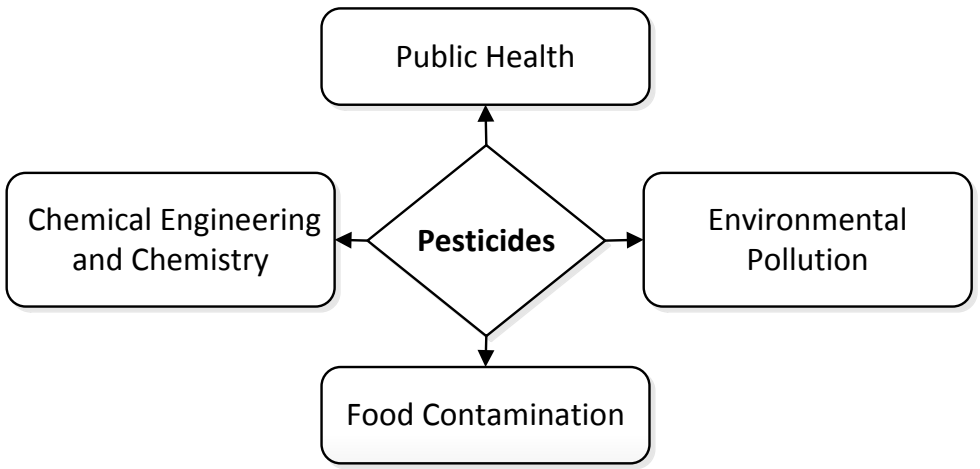

Figure **1:** Examples of research fields where pesticides are being studied

The fields presented in figure 1 are some of the areas where studies have been performed in order to evaluate the impact of pesticide use in different sectors of modern society.

In terms of environmental pollution, contamination of aquatic ecosystems by pesticide residues, for example, is still an active area of research [20], approaching topics such as the incidence of pesticides in surface and groundwater [22, 23], mobility and degradation of pesticides in soils [24] or the effects on the environment sectors such as fauna, biodiversity, etc. [25-27], among many others.

Within the food industry, food contamination by pesticides is a major concern which translates in several studies, some of them concerning the development and applicability of methodologies for identification and/or quantification of pesticides in food products [13, 28, 29] or the effect of the use of pesticides in the foodstuffs [30].

Other areas where pesticides are studied are chemistry and chemical engineering. Some examples of studies performed under these areas' scope are the development of detection, determination and control methods analysis [31-36] and characterization of the interaction between the pesticide and the environment [37] or pesticide degradation [38,39].

Studies about the health effects of pesticides on humans focus mainly on two aspects, acute toxicity (effects resulting from short-term exposure) and chronic toxicity (effects that result from extended exposure periods) [40].

Many studies can be found within the public health subject, especially regarding the possible association between pesticides and different diseases such as cancer [41-47], Parkinson's [48-50] or heart diseases [51-52].

Several other issues can also be found in the literature regarding this topic. Two examples are the connection between children's attention-deficit along with hyperactivity disorder and pesticide metabolites [53], or the association between sexual precocity and pesticide exposure [54].

Additional issues related to pesticides are addressed by other research fields, such as the area of toxicology [17, 55].

In water systems, the toxic action of pesticides is related to their chemical concentration and residence time/persistence in aquatic environments [56]. On one hand, the concentration depends of the amount poured into the environment; on the other hand, residence time is related to the capacity of the chemical to interact with suspended particles and sediments [57].

Regulatory frameworks have been developed to protect the health of humans and the environment resulting from exposure to pesticides. As a result of the persistence and toxic nature of these chemicals, the European Union has established maximum allowed concentrations of pesticides in drinking water. The set values are 0.1 μg L^{-1}, for any particular pesticide and 0.5 μg L^{-1} for the combination of all pesticides plus their degradation sub-products [58,59].

2.1.1. Paraquat

Paraquat, a quaternary ammonium herbicide, is widely used in agriculture due to its non-selective action, destroying green plant tissues on contact and by translocation within the plant [60] and until recently it held the largest share of the global herbicide market [19].

Paraquat was first synthesized in 1882 but its herbicidal properties were only discovered in 1955. This chemical was first commercially produced in 1961 by Zeneca Laboratories [61]

Paraquat is chemically identified as 1,1-dimethyl-4,4-bipyridinium dichloride and its structural formula is presented in Figure 2.

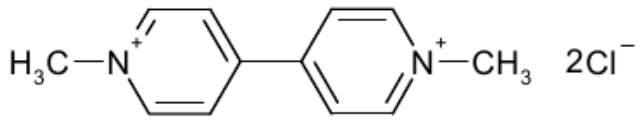

Figure 2: Structural formula of paraquat dichloride [62].

Paraquat allows a wide range of applications due its physical and chemical properties, such as high solubility in water, low vapour pressure and high binding potential, which makes it suitable for many agriculture uses [63]. Its mode of action is based on photosynthesis inhibition. In light-exposed plants, it accepts electrons from the photosystem I and transfers them to molecular oxygen, producing destructive reactive oxygen species.

Through this process, the oxidized form of paraquat is regenerated, becoming again available to bypass electrons from photosystem I to start the cycle again [64]. In this way, it kills green plant tissue on contact.

Despite its benefits, this compound is included in a priority list of herbicides of potential concern established for the Mediterranean countries by the European Union [65]. Paraquat was initially approved by the European Union in 2004 as an active plant protection substance. In 2007, however, this directive was annulled by the Court of First Instance [66]. Paraquat has been banned, or its use disallowed, in 32 countries (including the countries of the European Union), mainly due to health reasons. Many international organizations, such as the Rainforest Alliance or food giants like Dole have voluntarily banned it from their production systems [67].

This compound is extremely toxic and may pose potential environmental hazards to humans, often triggering cases of poisoning. When deliberately or accidentally ingested, its acute toxicity by oral route ranges from 4 to 40 mg kg^{-1}, being 35 mg kg^{-1} the generally accepted lethal dose [19, 40]. However, up to 3.5 mg kg^{-1}, it can be absorbed through the skin or respiratory route without acute toxic damage [19, 40, 60, 68]. Several possible health problems can be caused by exposure to this chemical such as irreversible damage to the lungs, which are the primary target [11], but a recent raising interest is related to an association of Parkinson's disease to paraquat or a combination of paraquat and fungicide exposures [68]. Since there is no antidote to reverse the effects

of this chemical on the human body, the current use of paraquat results in a health risk [12].

2.1.2. Chlorfenvinphos

Chlorfenvinphos, common name for 2-chloro-1-(2´,4´-dichlorophenyl)vinyl diethyl phosphate) is considered as a priority hazardous pollutant by the EU Water Framework Directive [58, 70].

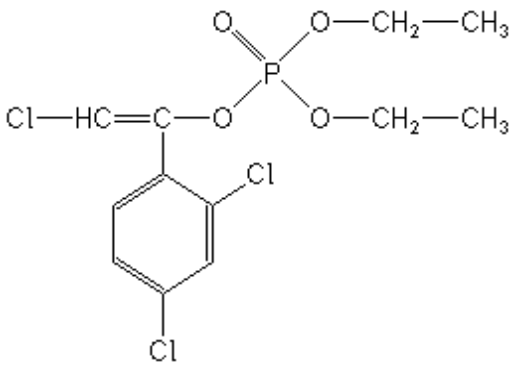

Figure 3: Structural formula of chlorfenvinphos [71].

This chemical is synthetic, not occurring naturally in the environment. Chlorfenvinphos was first registered in 1963 under the trade name Dermaton® [72] and is listed for uses in both agricultural and veterinary areas. As a veterinary chemical it is registered as a product for

ectoparasites' treatment in livestock [71]. In terms of application in agriculture, this chemical is used as an insecticide applied at soil level to control root-flies, rootworms and other soil pests [73]. It can also be used to deal with household pests such as flies, fleas and mice [74].

Some common trade names of this compound include Birlane®, Dermaton®, Sapercon®, Steladone®, and Supona® [75].

The pure compound is a colourless liquid with a mild odour. Insecticides commercially sold usually have around 90% of chlorfenvinphos. This chemical is easily mixed with acetone, ethanol, and propylene glycol; it is slowly broken down by water and is corrosive to metal [75].

This compound, similarly to the rest of organophosphate pesticides obtains its toxicity from its ability to inhibit acetylcholinesterase activity [76]. Having this ability, organophosphorus insecticides, in general, produce overstimulation of cholinergic neurotransmission, both centrally and peripherally, causing symptoms such as increased salivation, sweating, changes in blood pressure and heart rate, nausea, diarrhoea, headaches, muscle tremor, and, in high-dose situations, breathing difficulty, convulsions and death [58].

The neurotoxicity of these chemicals has been documented in accidental human poisoning cases and in epidemiological and animal model studies. Organophosphorus pesticides might also affect the immune response and induce apoptosis of immune cells [74].

2.1.3. Carbofuran

Carbofuran, common name for 2,3-dihydro-2,2- dimethyl-7-benzofuranyl-N-methylcarbamate, is a carbamate pesticide extensively used with agricultural purposes as a versatile, broad-spectrum systemic insecticide-nematicide, applied to the soil upon plant emergence, to control pests such as beetles, nematodes and rootworms [59, 77].

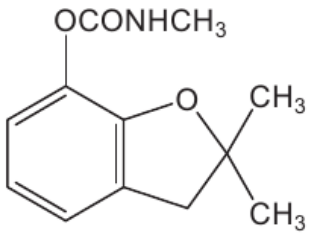

Figure 4: Structural formula of carbofuran [78].

This compound was first registered in the United States in 1969 and in Kenya in 1989 [79]. Carbofuran is sold worldwide as Furadan by FMC Corporation, in certain parts of the world it is sold as Curaterr by Bayer Crop Science. Additionally, it is sold by generic Chinese producers to Africa, Asia and Latin America [79]. In the European Union, this compound has been banned [80].

Carbofuran has been classified as highly hazardous due the extreme toxicity that it promotes [81]. This acute toxicity is thought to be related with the ability of carbofuran to inhibit acetylcholinesterase at synapses and neuromuscular junctions [82].

Although carbofuran is not chemically stable due to its easy hydrolysis in the environment, its residues are still frequently detected in groundwater due to its widespread usage and high mobility in soils [83]. Carbofuran is known to be more persistent than other carbamate or organophosphate insecticides [84].

2.2. Clays and iron oxides

Clays and metal oxides are the most abundant inorganic minerals in natural systems. The surface properties of colloidal clay and iron oxide particles play a major role in the formation, structure and strength of aggregates in soils [85]. These two groups of minerals can also be easily found in the inorganic content circulating in a drinking water network.

2.2.1. Clays

The term "clay" is used to refer to a naturally occurring material mainly composed of a small group of fine-grained crystalline particles of one or more minerals, commonly known as the clay minerals. In the group of clay minerals are kaolinite, smectite, montmorillonite, palygorskite, sepiolite, illite, chlorite, and mixed-layered clays [86].

Since the beginning of civilization, clay minerals have been object of great attention due to their abundance and unlimited potentials [87].

Some applications where clays or clay minerals are used include the process industries, agriculture, environmental remediation, engineering and construction, among many other miscellaneous applications [86, 88].

Several studies can be found in the available literature regarding clay and clay minerals properties and applicability in different areas [87, 89-98].

Clays have the ability to adsorb, retain, release, and incorporate into its structure a wide range of ions or molecules [99].

The applicability of clays is related to several general characteristics such as particle size and shape, surface chemistry, surface area and/or its charge and also other specific properties such as viscosity, colour, plasticity, dry and fired strength, absorption and adsorption, abrasion or pH. These properties make clay minerals suitable to perform certain functions and not just act as an inert component in the system [88]. For example, the extensive surface area of clays makes them excellent materials for catalysis applications, withholding toxic substances. On the other hand, in this field, clays can also be used as support for composites. The components of clays form stable suspensions in water which have been extensively used in drilling or tunnel piercing applications [99].

In the sorption research field, clays offer an attractive and inexpensive option for the removal of organic and inorganic contaminants [94].

These materials are perceived as effective natural adsorbents due to their small particle sizes, lamellar structures and negatively charged basal planes, i.e., the adsorption capacity of clays results from a relatively high surface area and a negative charge on their structure, which attracts and holds positively charged molecules through ion exchange or electrostatic attraction [60, 94].

Several recent studies involving clays and the adsorption of different compounds (methylene blue, carbaryl, endosulfan, 2,4,6-trichlorophenol, among others) can be found in the literature [100-106].

2.2.1.1. Kaolin

Kaolin, also known as China clay, is a mixture of different minerals, having as main component kaolinite, usually consisting of 85 to 95% [107]. In addition, kaolin frequently contains quartz, mica, feldspar, illite, and montmorillonite [107].

Kaolin can be found on all the continents of the world, exception made for Antarctica. However, even though it can easily be found, commercially viable deposits are scarce. For most industrial applications kaolin must be refined to increase its whiteness and purity, among other important commercial parameters [88]. Some of the properties of kaolin that account for many of their uses are:

- White or near white colour;

- Minimal layer charge;
- Low base exchange capacity;
- Pseudo-hexagonal flakes;
- Low viscosity.

Some applications where kaolin is used include paper production, where it is used as a coating material and in the paint, rubber, plastic, ceramic, and chemical, pharmaceutical, and cosmetics industries [107]. Kaolinite, the main constituent of kaolin, is made up of tetrahedral silica sheets alternated with an octahedral alumina sheets. Its structure consists of junctions of the tips of the silica tetrahedrons and the adjacent layers of the octahedral sheet forming a common layer. In the layer shared by the octahedral and tetrahedral groups, two-thirds of the oxygen atoms are shared by the silicon and aluminium, becoming 'O' instead of 'OH' [107]. This structure's charge is balanced but some charges occur on the edge of the kaolinite crystals due to broken bonds [88].

Kaolinite exhibits a low cation exchange capacity (in the order of 2–10 meq/100 g, depending on the particle size) but the rate of the exchange reaction is fast, almost instantaneous [107].

2.2.2. Iron oxides

Metal oxides/hydrous oxides can be found as naturally occurring discrete minerals or as coatings on other particles and exist in various amorphous and crystalline forms [108].

The surface of the metal oxides may be described as a two-dimensional net of neutral, positively and negatively charged groups, positioned at the interface [109]. In metal oxide suspensions, the charge development occurs by direct proton transfer, since the surface hydroxyl groups are ionisable [85]. Surface ionization reactions depend on the solution pH value. In acidic conditions, protonation of surface hydroxyls groups is enhanced while deprotonation is promoted in alkaline media. Surface charge and the formation of an electrified interface between particles and the aqueous medium (electrical double layer) is controlled by the pH and ionic strength of the solution in which oxide particles are dispersed [85].

Iron oxides are compounds easily found either in nature or synthesized in laboratory. Human kind is involved in iron oxide formation, not only as a living organism but also as a consumer of iron metal and iron oxides for various industrial purposes (Figure 5) [110].

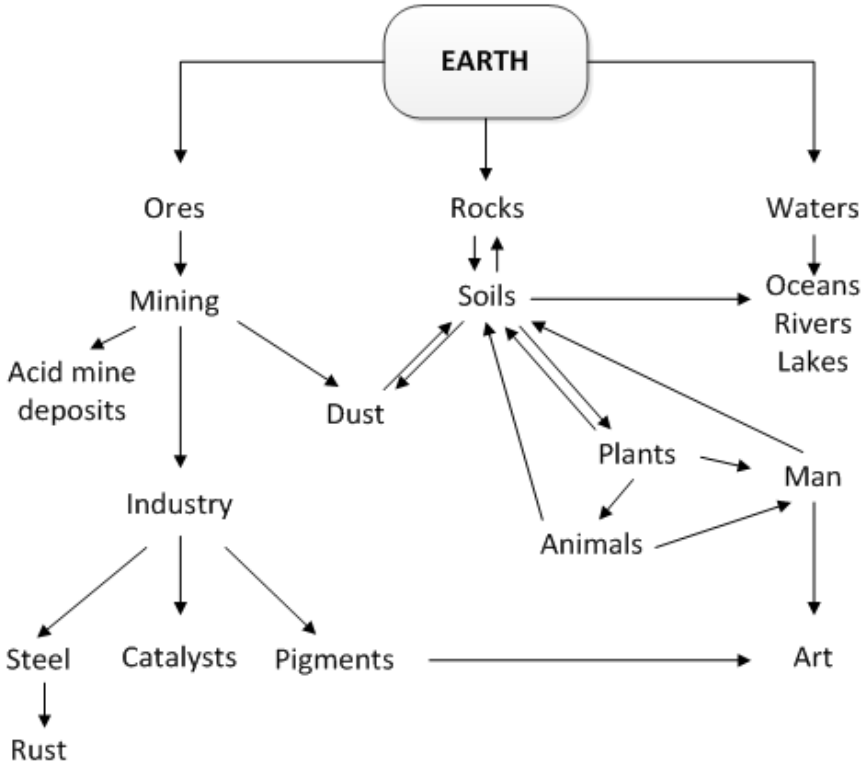

Figure 5: Iron oxide distribution in the global system [110].

There are six types of iron oxides, hematite (α-Fe_2O_3), magnetite (Fe_3O_4), maghemite (γ-Fe_2O_3), β-Fe_2O_3, ε-Fe_2O_3 and Wüstite (FeO) [111] and these compounds had been studied in a wide range of research fields (Figure 6) [110].

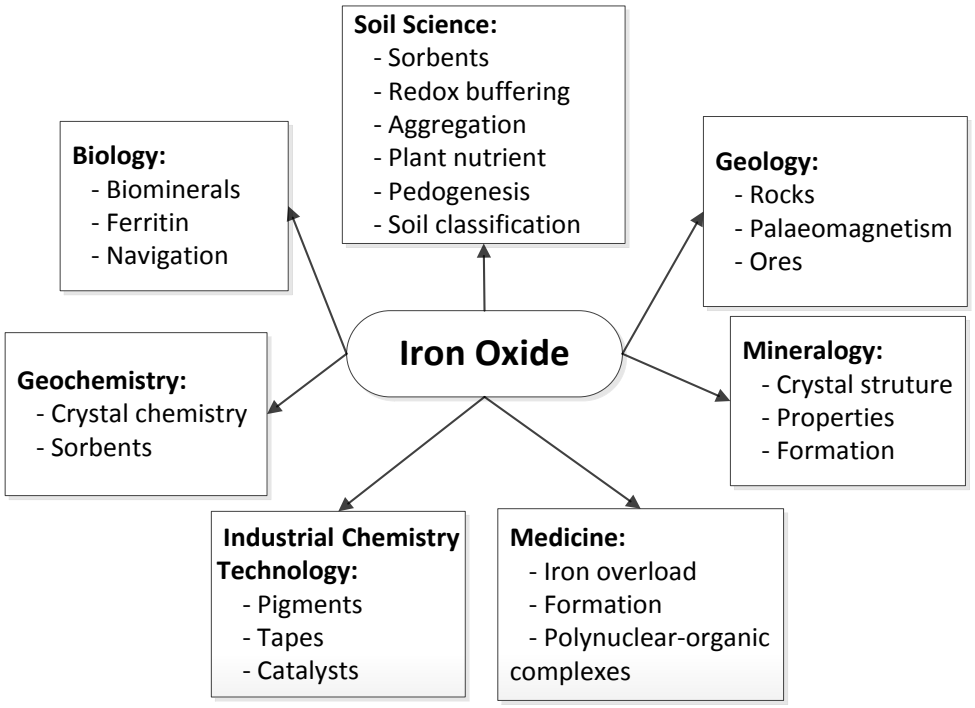

Figure 6: The multidisciplinary nature of iron oxide research [110].

The existence of various research fields using this material, gives an idea of its great applicability.

2.2.2.1. Hematite

Hematite is the oldest known iron oxide mineral and is extremely stable, often being the final stage of transformations of the other iron oxides, under ambiental conditions. Other names for hematite include iron (III) oxide, ferric oxide, red ochre and kidney ore [111].

Particles of this compound are known to have heterogeneous surfaces, including topographic features and defects, such that only certain portions of the surface will be reactive to any given geochemical process [112].

In the environment, hematite's presence is generalised, hosting several important bio-geochemical processes at surfaces or mineral/water interfaces. Due to its unique electronic and chemical properties, hematite is being increasingly used in catalytic, energy and environmental technologies. In both bio-geochemical processes and anthropogenic applications, surface chemistry of hematite plays an important role in charge accumulation, electron transfer, adsorption, and dissolution processes [113].

Recent studies regarding the use of hematite can be found in literature showing the still existing interest in this compound applied in different areas such as environmental science, nanomaterials, etc. [113-118].

2.3. Pesticide interaction with clays and iron oxides

The growing presence of pesticides in natural ecosystems has motivated research on adsorbent materials that could be used to address and prevent soil and water contamination.

Pesticide interaction with clay minerals, for example, has been studied for a long time. The initial papers on pesticide–clay interactions occurred in the 1970s and several studies have been performed since then [18].

Some of the work published in the latest years involving clays and iron oxides regards adsorption studies [104, 105, 119-121].

In this section a literature review is presented, concerning the interaction between the chosen pesticides and the two adsorbent materials selected.

2.3.1. Paraquat

As previously mentioned, paraquat has been extensively studied in several areas. Among the many types of studies performed and published in the latest years, sorption processes are some of the most common [40, 63, 122-125].

Available literature lacks on specific studies regarding the interaction between paraquat and iron oxides. Available studies generally concern the effect of iron oxides on the adsorption of paraquat by a particular sorbent. An example of this is the work of Pateiro-Moure *et al.*[65] on the sorption of paraquat by vineyard-devoted soils.

On the other hand, more information is available relating to the interaction between paraquat and clays in general [123, 126-128].

Tsai *et al.*, for example, have several studies regarding paraquat interaction with clays [11, 60, 129].

Even though numerous studies on the adsorption of paraquat onto clay minerals have been performed, the main focus has been the adsorption equilibrium and isotherm model. In contrast, published information on the kinetic modelling of paraquat sorption onto clay particles is limited [129].

Additionally, studies specifically involving paraquat interaction with kaolin are scarce. An example of the existing information on this subject is the study published in 1960's by Weber and Weed concerning the sorption phenomena of diquat and paraquat onto montmorillonitic and kaolinitic clay minerals [130].

2.3.2. Chlorfenvinphos and carbofuran

Even though chlorfenvinphos and carbofuran have been used in some sorption studies [20, 59, 131-134] there is a great lack of available information concerning the interaction between these pesticides and clays or iron oxide particles [131, 135-136].

2.4. Sorption equilibrium and kinetics

The transport and endpoint of a contaminant implicates complex mechanisms which are influenced by many processes, such as leaching, adsorption, chemical and biological decomposition [20]. This may constitute serious environmental issues concerning the fate and behaviour of these compounds and their sub-products on terrestrial and aquatic systems.

In an aquatic system, a contaminant's residence time and distribution between water and sediments (inorganic, organic and/or biological) depends on its capacity to interact with suspended particles and accumulated sediments [57].

The sorption phenomena of pollutants in aquatic systems are of great importance from the environmental point of view since they affect other processes such as transport, degradation or bioaccumulation, which influence the mobility and the ultimate fate of pollutants like pesticides [137].

2.4.1. Sorption isotherms

The sorption of a chemical onto a solid from an aqueous solution can be defined as the outcome of a reversible reaction (adsorption–desorption)

in which equilibrium is achieved when the concentration of the chemical in the two phases become balanced [57].

At constant temperature, the relation between the amount of solute adsorbed in the solid and its concentration in bulk liquid is known as adsorption isotherm [138-139]. Sorption isotherms are used to quantify the maximum amount of chemical that a solid phase can adsorb and the affinity between solute and adsorbent.

The most common sorption isotherms are represented by Langmuir and Freundlich equations [140]. These models may be described by equations 1 and 2 [141-142].

$$q_e = \frac{q_{max} K_L C_e}{1 + K_L C_e} \quad (1)$$

$$q_e = K_F C_e^{1/n} \quad (2)$$

In these equations K_L is related to the energy of adsorption; K_F is related to adsorption capacity and n_F is related to the adsorption intensity [143].

The Langmuir model assumes that equilibrium is achieved when an adsorbent's monolayer is saturated with solute molecules [20]. It also assumes that the adsorption energy of each molecule is the same for all surface sites and independent on the degree of surface coverage. Adsorption takes place in specific sites that after being occupied will not

permit further adsorption to occur [142]. Parameters q_{max} and K_L are used to describe the sorption capacity of the material [140].

On the other hand, the Freundlich isotherm model assumes that adsorption occurs on heterogeneous surfaces with distinct adsorption energies and different active sites. The parameter n_F provides information on the adsorption process favourability while the constant K_F, as previously referred, is related to the adsorption capacity of the adsorbate [103]. This model, despite its empirical nature, is quite precise when it comes to describe systems where adsorption occurs in heterogeneous surfaces [100].

2.4.2. Sorption kinetics

Sorption kinetic studies are a useful tool to quantify the solute uptake rate which controls the residence time of the solute at the solid-liquid interface [142]. Additionally, this type of studies can be applied to better comprehend the limiting step of the mass transfer process [144].

Sorption kinetics is also an important issue for many aspects of surface chemistry, from the understanding of sorption mechanisms to more practical issues such as the removal of pollutant components from solutions [145].

Equilibrium and sorption kinetics have been extensively studied in the past [146] and a wide number of adsorption processes for pollutants

have been studied [57, 104, 147-149] in an attempt to find a suitable explanation for the mechanisms and the quantification of its kinetics, so that environment protective solutions could be developed [104, 150].

Several models can be used to quantify the kinetics of sorption processes. Various approaches have been proposed and differentiated by the processes that are considered to be governing the overall sorption rate [144, 150-151]. The following types of models can be used to describe sorption phenomenon [144]:

- Apparent (or “observable”) adsorption rate models
- Film diffusion models
- Intra-particle diffusion models
- Combination of film and intra-particle diffusion models

In order to investigate the rate of sorption and its constants, two apparent adsorption models were applied, pseudo-first and pseudo-second order models which are as follows:

The pseudo-first order equation for the liquid-solid adsorption system is generally expressed as [145, 152]:

$$\frac{dq_t}{dt} = k_1 (q_e - q_t) \tag{3}$$

Eq. (3) integrated from $t = 0$ to $t > 0$ and then rearranged gives place to the following semi-log linear time dependent function:

$$log(q_e - q_t) = log(q_e) - \frac{k_1}{2.303} t \quad (4)$$

Kinetic parameters (***k₁*** and ***qₑ***) are determined from slope and intercept of plots of **log(q_e–q_t)** ***vs*** **t.**

The pseudo-second order differential equation is given by [153, 154]:

$$\frac{dq_t}{dt} = k_2 (q_e - q_t)^2 \quad (5)$$

Separating the variables in Eq. (5) gives:

$$\frac{dq_t}{(q_e - q_t)^2} = k_2 dt \quad (6)$$

Integrating this for the boundary conditions $t = 0$ to $t = t$ and $q_t = 0$ to $q_t = q_t$:

$$\frac{1}{(q_e - q_t)} = \frac{1}{q_e} + k_2 t \quad (7)$$

Eq. (7) can be rearranged to obtain a linear form in terms of **t/q_t**:

$$\frac{t}{q_t} = \frac{1}{q_e} t + \frac{1}{k_2 q_e^2} \quad (8)$$

The constants can be determined by plotting ***t/q_t*** against ***t***.

Even though these semi-empirical adsorption models are widely used, it is important to be aware of their conceptual limitations. External liquid film and intra-particle diffusion are dismissed in the above equations, even though these steps may be significant in the overall adsorption processes [144].

In the case of the research studies here presented, no adsorption internal diffusion models were applied due to the extreme difficulty to obtain data regarding intra-particle sorption processes. Thus, it is here considered that the overall adsorption rate follows a model that describes the so-called “observable” global adsorption process.

Such models assume an average uniform concentration of contaminant inside the sorbent and, therefore, they describe the overall process as a series of two steps:

- Transport from the bulk liquid to the sorbent’s surface;
- Interaction of the contaminant with the solid sorbent.

The last step is represented by equation 8 (considering the case of a second order model).

2.4.3. Mass transfer coefficients and correlations

In many chemical and biochemical processes, mass transfer from or to solid particles suspended in agitated liquids is very important. Some of

these processes are adsorption, crystallization, fermentation, slurry reactions and wastewater treatment [155].

The overall rate of mass transfer of the solute to an adsorbent's active site is based on three steps [144, 153]:

- Diffusion across the liquid surrounding the external surface of adsorbent particles, i.e., external mass transfer;
- Solute migration through the liquid contained in the pores and/or along the pore walls, the so-called internal diffusion;
- Interaction (adsorption/desorption) between the solute and the active sites.

In the present study, as previously mentioned in section 2.4.2, steps 2 and 3 are combined in only one step, described by equations such as Eq. (8).

The first step represents what happens to the contaminant (solute) from the bulk liquid to the surface of the sorbent – external mass transfer. The rate at which this phenomenon occurs depends on:

- The concentration gradient of the solute between the bulk liquid and the solid;
- The solid's mass transfer area available for the solute-sorbent interaction;
- The diffusivity (or molecular diffusion) of the solute in the liquid;

- The concentration profile in the boundary layer next to the solid surface (which is related to the prevailing hydrodynamic pattern which is dependent on the flow regime and other local properties).

Since molecular diffusivities do not describe the transport in turbulent flow regimes, semi-empirical mass transfer coefficients are used here to quantify transport rates through the following rate equation [139]:

$$J = k_m A(C_b - C_s) \tag{9}$$

The assessment of mass transfer coefficients is very important since this parameter determines the rate at which equilibrium is approached and controls the time required for a given separation to occur [156]. For example, the higher the value of the coefficient, the faster mass transfer occurs, the quicker equilibrium will be reached and vice-versa [139].

Mass transfer coefficients can be, in practical terms, predicted from semi-empirical correlations based on a significant amount of mass transfer data obtained in similar situations [139].

Among the available correlations for agitated liquids, the equation of Boon-Long [157] was selected to predict mass transfer coefficients in the experimental setup and assess the effect of the external mass transport on the adsorption kinetics.

$$Sh = 0.046\ Re^{0.283}\ Ga^{0.173}\ U^{-0.011}\ \left(T/d\right)^{0.019}\ Sc^{0.461} \tag{10}$$

From the above equation, mass transfer coefficient can be expressed in terms of dimensionless numbers, $K_{LS} = f(Sh,Re,Ga,Sc)$. The dimensionless numbers that intervene in Eq. (10) are expressed by:

$$Sh = \frac{K_{LS}\, d}{D_V} \tag{11}$$

$$Re = \frac{d\, T\, \omega\, \pi}{v} \tag{12}$$

$$Ga = \frac{\rho^2\, g\, d^3}{\mu^2} \tag{13}$$

$$Sc = \frac{\mu}{\rho\, D_V} \tag{14}$$

In previous equations Sh, Re, Ga and Sc represent the Sherwood, Reynolds, Gallileo and Schmidt dimensionless numbers, respectively.

Other symbols stand for mass transfer coefficient in the liquid-solid interphase ($\mathbf{k_{LS}}$), particle diameter (**d**), diffusivity of the solute in the liquid ($\mathbf{D_v}$), vessel diameter (**T**), stirrer angular velocity ($\boldsymbol{\omega}$), kinematic viscosity ($\boldsymbol{\nu}$), density of liquid ($\boldsymbol{\rho}$), gravitational constant (**g**), viscosity of the liquid ($\boldsymbol{\mu}$) and in equation 10, **U** regards the solid concentration.

Chapter 3.

Experimental Procedures

3.1 Characterization of natural source clay

The clay used in these experiments was obtained from an unknown natural source. Even though it was suspected to be essentially kaolin, a proper characterization was needed. Chemical and mineralogical analyses were performed at LNEG (Laboratório Nacional de Energia e Geologia), in order to assess the composition of the selected substance. The characterization of the clay, concerning elemental quantification, was determined by X-Ray Fluorescence analysis. In terms of mineralogy, samples were subjected to a semi-quantitative mineralogical analysis by X-Ray Diffraction.

Textural characterization of the samples was based on the analysis of nitrogen sorption isotherms measured at 77 K in a Quantachrome NOVA 4200e apparatus [158]. BET surface area and micropore volume were calculated using the BET equation and the t-method, respectively [159]. Total pore volume, i.e. the sum of micropore and mesopore volumes, was determined from the nitrogen adsorption isotherms at a relative pressure of 0.99. The mesopore volume was obtained by subtracting the micropore volume from the total pore volume. Pore size distributions were obtained from the desorption branch of the isotherm using the Barrett, Joyner and Halenda (BJH) method [160]. Particle sizing was determined in a Coulter Counter LS 230 with small volume model.

3.2. Assays performed with paraquat

3.2.1. Adsorption and desorption assays with suspended particles

Adsorption experiments were carried out in stirred batches, using two combinations of adsorbents: kaolin (2 g L^{-1}) and a mixture of kaolin/hematite ($P_{K/IO}$= 2:1, with 2 g L^{-1} of kaolin) that were put in contact with 100 mL of paraquat solution with an initial solute concentration of 50 mg L^{-1}. The assays were conducted at an agitation speed of 440 rpm using a multi-point magnetic stirrer (IKAMAG® RO 15 POWER) for a maximum period of 24 hours at room temperature (23 ºC). Overtime, suspension samples were filtered using nylon syringe filters 0.45 µm, 25 mm Ø (VWR International), and analysed by liquid chromatography (HPLC) in order to measure the concentrations of paraquat remaining in the solution. It was used a Purospher®STAR LiChroCART® RP-18 endcapped (240 mm × 4 mm, 5 µm) reversed phase column with a JASCO MO-2015 Plus multi wave-length detector, in a JASCO equipment. Analytical conditions were implemented according to the method described by Santos *et al.* [161]: mobile phase consisting of 80% HFBA 10 mM and 20% acetonitrile, flow rate of 1 mL min^{-1}, injection volume of 99 µL and a wavelength of 259 nm.

For desorption studies, contaminated kaolin and mixed particles obtained from the adsorption assays were re-suspended in 100 mL of

deionised water with an agitation speed of 440 rpm at constant temperature for 60 hours. Samples were processed as previously described.

3.2.2. Adsorbent concentration effect on the adsorption phenomena

In order to assess the effect of adsorbent concentration on the adsorption process, experiments were carried out in stirred batches, using several concentrations of adsorbent - kaolin (1; 1.5; 2; 3 g L^{-1}) and a kaolin/hematite mixture (1:0.5; 1.5:0.75; 2:1; 3:1.5 g L^{-1}:g L^{-1}) - that were tested against 100 mL of paraquat solution, with an initial solute concentration of 50 mg L^{-1}. The assays were all conducted in duplicate in a multi-point magnetic stirrer at 440 rpm for a period of 24 hours, at room temperature (23 ºC). Collected samples were processed and analysed by HPLC, as described in the previous section.

3.2.3. Agitation speed effect on the adsorption phenomena

The procedure described above was also adopted in this study using two more agitation speeds (330 and 550 rpm) in a multi-point magnetic stirrer (IKAMAG® RO 15 POWER). The adsorbent dosage used was 2 g L^{-1} of

kaolin and a mixture of kaolin and iron oxide ($P_{K/IO}$= 2:1) and it was tested against 100 mL of paraquat solution (initial concentration: 50 mg L^{-1}) for a period of 4 hours, at room temperature. Samples were taken overtime, filtered using nylon syringe filters 0.45 µm, 25 mm Ø (VWR International) and analysed by HPLC, following the methodology described in section 3.2.1.

3.2.4. Initial pH effect on paraquat adsorption on kaolin particles

This assay was conducted similarly to the one applied to determine paraquat adsorption kinetics in suspended particles. A dosage of 2 g L^{-1} of kaolin particles was suspended in 100 mL of paraquat (50 mg L^{-1}). The assays were conducted at 440 rpm using a multi-point magnetic stirrer (IKAMAG® RO 15 POWER) for a period of 240 minutes at room temperature (23 ºC).

Initial pH of the paraquat solution was adjusted to two values (3 and 7) using nitric acid (65 %) from Emsure and sodium hydroxide solution (0.1 M) prepared using sodium hydroxide salt from Pronalab. Samples were taken over 240 minutes, processed and analysed by HPLC, following the methodology described in section 3.2.1.

3.2.5. Preparation of standard solutions and adsorption isotherm procedure

An aqueous stock solution of 200 mg L^{-1} of paraquat dichloride was prepared using deionised water, previously filtrated with 0.45 µm nylon filter membranes 47 mm Ø from Supelco. From this stock solution, standard solutions of 5, 10, 20, 30, 40, 50, 60, 70, 80, 90 and 100 mg L^{-1} were prepared using deionised water.

Based on the adsorption assays, an equilibrium time was set and the isotherms were determined, using 12 well polystyrene microplates (Orange Scientific), varying the mass ratio of chemical and particles. A constant mass of adsorbent (10 g L^{-1} of kaolin and 5 g L^{-1} of iron (III) oxide and a mixture of the kaolin/hematite ($P_{K/IO}$= 2:1)) was exposed to 1.5 mL of paraquat concentration (concentrations between 5 and 100 mg L^{-1}) during 4 hours, using an agitation speed of 150 rpm with an orbital mixer (CERTOMAT® BS-1, Sartorius AG, Germany). Each well represented one ratio and the assays were conducted in duplicate. These experiments included a control to check if there was any chemical retention by the polystyrene of the microplate and a blank. The blank was the water resulting from the aqueous suspensions filtration and was used to attest that it did not contain any compound that could interfere in the identification and/or quantification of the chemical under study.

These experiments was carried out at two temperatures (8 and 28 ºC) in order to assess this parameter's influence in the final results.

3.2.6. Formation and characterization of adhered deposit

In order to produce adhered deposits, a reactor containing two litres of sterile suspension of kaolin (2 g L^{-1}) or mixed suspension ($P_{K/IO}$= 2:1) was left re-circulating at 7.8 L min^{-1} in a flow cell apparatus based on the one reported by Teodósio *et al.* [162], for periods of twenty and ten days, respectively, at room temperature (23 ºC), as shown in Figure 7a.

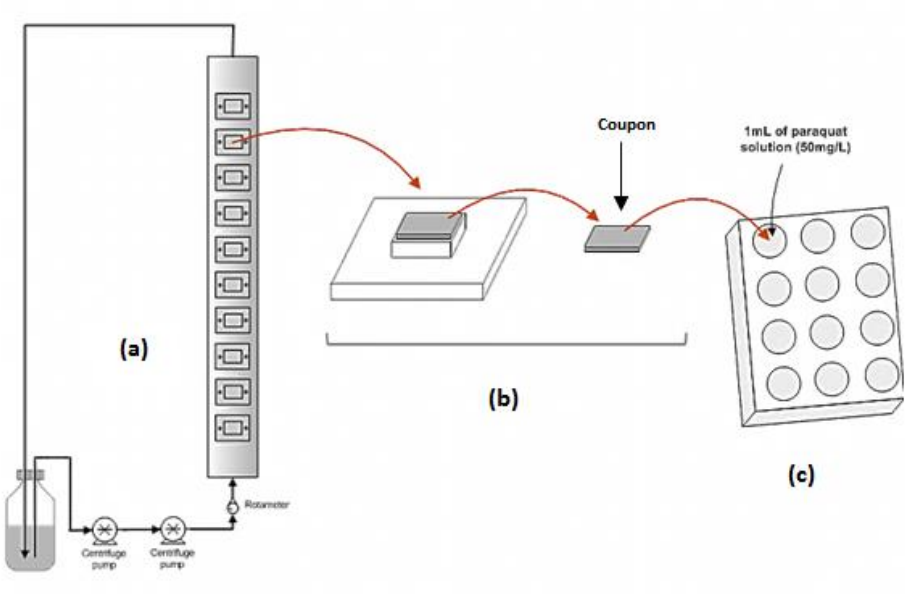

Figure 7: Schematic representation of the experimental setup: deposit formation unit (a); removal of coupons from its holder (b); apparatus for chemical exposure to paraquat (c)

Subsequently to deposit formation, representative samples were analysed to characterize the deposit in terms of thickness, wet and dry

mass. To determine wet deposit thickness, a digital micrometer device (VS-30H, Mitsubishi Kasei Corporation) was used following the method described by Teodósio *et al.* [163]. The wet mass of the deposits was determined by weighing the coupons before and after deposit formation. Immediately after being collected, each coupon was weighed and the deposit thickness was measured. Then the coupons were dried in a desiccator until constant mass was reached. Dry mass was given by comparing the weight of clean coupons and the weight of the same coupons with deposit after drying [164].

3.2.7. Particle and deposit characterization - scanning electron microscopy

With the purpose of analyzing the morphological characteristics and composition of particles and deposits, a JEOL JSM 6301F scanning electron microscope equipped with an EDS micro-analysis system (Oxford INCA Energy 350) was used. Adhered deposit samples of kaolin and kaolins/hematite mixture were analyzed at CEMUP (Centro de Materiais da Universidade do Porto).

3.2.8. Paraquat adsorption onto adhered deposits

After deposit formation, the coupons were removed from its holders (Figure 7b), weighed and transferred to a 12 well polystyrene microplates

(Orange Scientific) were they would be exposed to 1 mL of paraquat solution with an initial concentration of 50 mg L^{-1} (Figure 7c). Each coupon represented one time point and samples were taken over 24 hours. Samples were filtered using VWR International nylon syringe filters 0.45 µm, 25 mm Ø, and analysed according to the analytical method previously described in section 3.2.1.

3.2.9. Agitation speed effect on the adsorption phenomena (adhered deposits)

Due to defragmentation of flow cell deposits when studied with agitation, substitute deposits were formed by sedimentation in a 12 well polystyrene microplates (Orange Scientific) using particle suspensions of 10 g L^{-1} of kaolin or 15 g L^{-1} of kaolin/iron (III) oxide mixture ($P_{K/IO}$= 2:1 with 10 g L^{-1} of kaolin) that were left to dry in a desiccator. After constant mass was achieved, 1 mL of paraquat solution (50 mg L^{-1}) was added to each well.

The assays were conducted in duplicate for the two types of deposits, in an incubator CEROMAT BS-1 from SARTORIUS, using two agitation speeds (0 and 150 rpm). Each well represented one time point, and the samples were taken over a 24 hour period. Samples were processed and analysed by HPLC, as previously described.

3.2.10. Adsorption kinetic parameters

The study of adsorption kinetics is a useful tool to describe and translate the solute uptake rate by gaining a quantified insight on the adsorption reaction mechanisms which involve mass transfer, diffusion and surface reaction phenomenon during the adsorption process [151, 165].

The experimental data obtained from the adsorption studies were adjusted using pseudo-first and pseudo-second order kinetic models, previously described in section 2.4.2. Kinetic parameters were determined by one of two ways: plotting $\mathbf{\log(q_e - q_t)}$ against **t**, in the case of the pseudo-first order model and $\mathbf{t/q_t}$ against **t** for pseudo-second order model.

It should be stressed once again that the kinetic model equations, which are commonly used in adsorption studies, represent overall non-structured models where detailed steps of adsorption such as intra-particle diffusion are not explicitly described and, as such, the resulting kinetic parameters should be considered “observable” or “apparent” coefficients that encompass both the specific physico-chemical interactions and the mass transfer effects.

In order to quantify the maximum adsorption capacity of the studied adsorbents for the removal of paraquat from aqueous solutions, in a set of pre-determined conditions, data collected from the isotherm assays were adjusted by the Langmuir and Freundlich models.

The model adjustment was assessed by considering two factors [142], correlation coefficient (R^2) and normalized standard deviation (SD) given by:

$$SD(\%) = \sqrt{\frac{\frac{\left(q_{exp} - q_{calc}\right)^2}{q_{exp}}}{n-1}} x100 \quad (15)$$

3.3. Preliminary assays performed with chlorfenvinphos

3.3.1. Chlorfenvinphos adsorption onto kaolin suspensions

Adsorption assays were carried out mixing 70 g L^{-1} of kaolin with 100 mL of a chlorfenvinphos solution (initial concentration: 10 mg L^{-1}). Chlorfenvinphos PESTANAL®, analytical standard (Fluka) was supplied by Sigma-Aldrich. Suspended particles were placed in 100 mL glass shots left shaking in a multi-point magnetic stirrer (IKAMAG® RO 15 POWER) at 550 rpm, for a total of 6 hours at room temperature (23 ºC), samples being taken during this period. The assays were conducted in duplicate and each sample was filtered using Fibre Glass syringe filters 1 µm, 25 mm Ø (Frilabo collection), and analysed by liquid chromatography (HPLC) in order to measure the concentrations of chlorfenvinphos remaining in the solution. It was used a Purospher®STAR LiChroCART® RP-18 endcapped (240 mm × 4

mm, 5 µm) reversed phase column with a JASCO MO-2015 Plus multi wave-length detector, in a JASCO equipment. Analytical conditions were implemented according to the method described by Oliveira [166]: mobile phase consisting of 70% acetonitrile and 30% water, flow rate of 1 mL min^{-1}, injection volume of 99 µL and a wavelength of 240 nm.

3.3.2. Agitation speed, initial pH and temperature effects on chlorfenvinphos adsorption to kaolin particles

These assays were conducted similarly to the one described in section 3.3.1. It was used 7 g of kaolin particles suspended in 100 mL of chlorfenvinphos solution (initial concentration: 10 mg L^{-1}). The assays were conducted at 550 rpm using a multi-point magnetic stirrer (IKAMAG® RO 15 POWER) for a period of 6 hours at room temperature (23 ºC).

To evaluate the effect of the agitation speed two other velocities were applied, 330 and 770 rpm.

Regarding the effect of initial pH, chlorfenvinphos solution was adjusted to three different pH values (3, 7 and 10) using nitric acid (65 %) from EMSURE and sodium hydroxide solution (0.1 M) prepared using sodium hydroxide salt from PRONALAB.

To assess the influence of the temperature, three different temperatures were used 5, 25 and 37ºC.

For all the assays, samples were taken over a period of 6 hours, processed and analysed by HPLC, following the methodology described in section 3.3.1.

3.4. Preliminary assays performed with carbofuran

3.4.1. Carbofuran adsorption onto kaolin and kaolin/hematite mixture suspensions

Adsorption experiments were based in a procedure presented by Hsieh *et al.* [167]. These assays were carried out mixing 5 g of kaolin (or 5 g of kaolin plus 2.5 g of hematite) with 10 mL of a carbofuran solution (2.5 mg L^{-1}). Carbofuran PESTANAL®, analytical standard (Fluka) was supplied by Sigma-Aldrich. Suspended particles were placed in 50 mL polystyrene tubes and left shaking at 550 rpm in an IKA KS 130 BASIC orbital shaker, for a total of 24 hours, at room temperature (23 ºC), samples being taken during this period. The assays were conducted in duplicate for the two types of suspended particles. Each sample was collected, centrifuged in a EPPENDORF 5810 R centrifuge, at 4000 rpm for 10 min, filtered using PTFE syringe filters 0.45 µm, 25 mm Ø supplied by VWR International.

Samples were analysed by liquid chromatography with a JASCO MO-2015 Plus multi wave-length detector, in a JASCO equipment. The

analytical method implemented consisted of a chromatographic separation achieved by a Purospher®STAR LiChroCART® RP-18 endcapped (240 mm × 4 mm, 5 μm) reversed phase column supplied by VWR, using a mobile phase of 70% (v/v) of water and 30% (v/v) of acetonitrile, at isocratic conditions, with a flow rate of 1 mL min^{-1}. The calibration curve was performed by direct injection of eight standards, from 0.1 to 100 mg L^{-1} of carbofuran. The quantification of carbofuran was recorded at 220 nm with a retention time of 15.7 min. The value of the correlation coefficient was 0.9996. Precision was evaluated through the repeatability of six injections of the same analytical standard, variation coefficients were very low (1.6%, 0.2% and 1.4% for 10, 50 and 100 mg L^{-1}, respectively). Accuracy was evaluated by comparison with reference materials, for which the concentration of carbofuran is known. Accuracy was expressed as percentage of recovery and was 100 % for 10, 50 and 100 mg L^{-1} of carbofuran.

3.4.2. Initial pH effect on carbofuran adsorption on kaolin particles

The same procedure as the described above was adopted in this study. It was used 5 g of kaolin (or 5 g of kaolin plus 2.5 g of hematite) with 10 mL of a carbofuran solution (2.5 mg L^{-1}).

Three pH values were studied, 3, 7 and 10. The pH of the carbofuran solution was adjusted to the intended values using nitric acid (65%) from

Emsure and sodium hydroxide solution (0.1 M) prepared using sodium hydroxide salt from Pronalab. Samples were taken at 18 and 24 hours of contact time, processed and analysed as reported in the previously section.

3.5. Statistical analysis

The experimental data were statistically analysed using MS Office Excel software (Microsoft Office 2010). The mean and standard deviation within samples were determined for all experiments. Significant difference between pairs of data was tested using the Student's t-test. Statistical significance was considered at a confidence level of 95%.

Chapter 4.

Results and Discussion

4.1. Characterization of natural source clay

In order to confirm the nature of the clay used in this research study, several analyses were performed regarding chemical and mineralogical composition and particle characteristics.

4.1.1. Chemical analysis

One of the issues addressed concerning the characterization of the sampled clay was the identification and quantification of its constituents. According to the data provided by LNEG, it was determined that samples were mostly constituted by Al_2O_3 and SiO_2. The remaining components were detected in trace amounts.

The results provided LNEG are presented in Table 3 and given as mass percentage.

Table 3: Composition and quantification (in percentage) of the clay sample constituents.

Constituents	Sample Composition (%)
SiO_2	49.11
Al_2O_3	33.61
Fe_2O_3	1.43
MnO	< 0.02
CaO	0.05
MgO	0.27
Na_2O	< 0.20
K_2O	2.53
TiO_2	0.38
P_2O_5	0.10
Volatile matter	12.26

4.1.2. Mineralogical analysis

As previously mentioned, kaolin is an aluminium-silicate mineral belonging to the class of clays, comprising more than one mineralogical species, the dominant one being kaolinite [168]. In addition to kaolinite, this type of clay frequently contains quartz, mica, feldspar, illite, and montmorillonite [107].

The data obtained from the mineralogical analysis made it possible to confirm the type of clay used in the research experiments. According to the data provided by the analysis, kaolinite represents 77% of the total

components of the sample and the remaining constituents detected were expectable considering the type of clay. The results provided LNEG, are presented in Table 4 and given as percentage.

Table 4: Mineralogical composition and quantification of the clay sample constituents.

Constituents	Kaolinite	Mica	Quartz	Feld K	Hematite
Sample Composition (%)	*77*	16	3	4	Traces

4.1.3. Textural characterization and granulometric analysis

The applicability of clays is deeply related to their characteristics. Parameters like particle size, shape and surface area, among many other important properties, make clay minerals suitable to perform certain functions and not just act as an inert component in the system [88]. Some of these parameters were determined, in order to better characterize the raw material used in the experiments.

The analyses of textural properties of the clay samples provided a BET surface area of 13.8 $m^2\ g^{-1}$. Moreover, the particles exhibited a pore radius of 21 Å and a total specific pore volume of 0.068 $cm^3\ g^{-1}$ which represents the mesopore volume since micropore existence was not detected. Particle size analysis gave an average particle diameter of 15 µm.

Comparing the information from the characterization of clay used in this experimental research with data collected from the literature, the value obtained for the BET area is consistent with several previous studies [89, 149, 169-170]. Although different values can also be found in other studies, such as 20.2 $m^2 g^{-1}$ [171] or 33.5 $m^2 g^{-1}$ [172], for the BET surface area, they exhibit the same order of magnitude of the present one. On the topic of average particle size, there is no consensus in the published literature, with distinct values being provided (i.e. 0.77 µm [89], 2.37 µm [170], 9.6 µm [173]). These disparities in average particle size values may be related to different degrees of purity of the kaolin samples or the level of particle aggregation.

4.2. Paraquat assays

4.2.1. Adsorption/desorption studies performed with suspended particles

Applying the methodology described in section 3.2.1, a reduction of approximately 18% (from 50 mg L^{-1} to 41 mg L^{-1}) in the paraquat concentration was obtained from the exposure of the suspended particles (kaolin and particle mixture) to the herbicide under the set conditions.

From the data presented in Figure 8, it is evident, for both kaolin and mixed kaolin/hematite suspensions, that the paraquat adsorption reaches

a plateau very rapidly. Considering standard deviations and statistical analysis (P>0.05), beyond this point no significant variations were registered. After one minute of chemical/particle interaction the plateau is reached, i.e., equilibrium is almost instantaneous.

Paraquat adsorption behaviour registered in the studied situations is supported by other studies available in the literature [68, 165, 174].

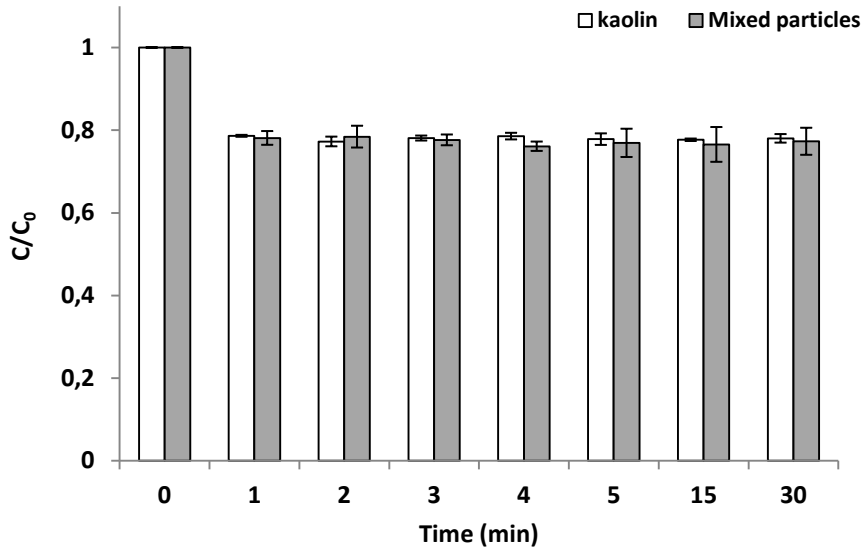

Figure 8: Variation in paraquat concentration overtime (30 minutes) for kaolin (2 g L^{-1}) and mixed ($P_{K/IO}$= 2:1) suspensions exposed to a 50 mg L^{-1} paraquat solution (23 ºC, 440 rpm, pH 6). Means with standard deviations for three replicates are illustrated.

Clay adsorption capacity comes as a result of the relatively high surface area and a net negative charge on its structure, which attracts and holds cations [94]. In the particular case of kaolin, its particles are believed to carry a constant structural negative charge as a result of the substitution

of Si^{4+} by Al^{3+} in the silica layer, whereas the charge on the alumina face and on the edges are pH dependent due to the protonation/deprotonation of the exposed hydroxyl groups [169].

Paraquat is known to adsorb strongly on clay minerals [129]. The high affinity between paraquat and clay minerals is related to its high polar nature [175]. Paraquat molecules bear two charges which suggest that the main driving force for adsorption is electrostatic and that the adsorption process can be assumed to be completed when the surface charge is neutralized [174]. The cationic nature of the chemical promotes the binding between the herbicide and negatively-charged surfaces of clay [176].

The obtained results suggest that there are no restrictions over the mass transfer process (either external or internal) that might prevent paraquat molecules from quickly reaching and interacting with the active sites of the adsorbent. From the instant paraquat contacts with the adsorbent, an interaction occurs, promoting the neutralization of the charges in the mineral particles.

Several types of forces may be involved in the adsorption of paraquat, particularly Coulombic forces. However, additional forces seem to contribute to the binding in the interlayer spacing, such as Van der Waals forces and charge-transfer complexes [175].

In these assays, the hematite added to kaolin had no apparent effect on the maximum amount of paraquat adsorbed but caused an enhancement in the adsorption kinetic constant. This suggests that iron (III)

oxide may not act as an adsorbent but presents itself as a facilitator in this adsorption process, under the applied conditions. In fact, the interaction between paraquat and iron oxides is usually low [123, 175]. The role of iron (III) oxide as facilitator can be explained by the formation of a complex kaolin-iron oxide whose charge becomes more negative, accelerating the adsorption of positively charged paraquat molecules, as demonstrated by Pateiro-Moure *et al.* [177]. Another possibility could be the occurrence of changes in the surface charge properties of the hematite particles but to attest this hypothesis, further studies on the surface charge properties [108, 178, 179] have to be performed.

Pesticide desorption processes have been less studied than adsorption. On the other hand, the degree of irreversibility of the adsorption is very important when it comes to the determination of the mobility of any pesticide in the aquatic environment [137].

Desorption assays indicate that this phenomena may be neglected in the experimental conditions applied, since there was not detected any release of chemical from the contaminated particles. This outcome is supported by the results obtained by Santos *et al.* [180] in a study concerning the adsorption of paraquat on deposits from drinking water networks. The inexistence of paraquat desorption or negligible paraquat removal can be explained by the strong adsorption capacity attributed to binding in the inter-layer of clay minerals, by which, to some degree of coverage, no paraquat could be analytically detected in solution [5]. Moreover, adsorption is usually restricted to the amount corresponding to the cation exchange capacity, the occurrence of a charge reversion being

unlikely [175]. Based on this information the result obtained with the desorption studies was somewhat expectable.

4.2.1.1. Data Fitting and adsorption kinetic parameters

The parameters of adsorption kinetics can be very useful to describe the rate of solute uptake and consequently evaluate the residence time of the solute at the solid-liquid interface. In this section, the kinetics of paraquat adsorption onto suspended particles was analysed using pseudo-first and pseudo-second order models to determine kinetic parameters. The values of kinetic parameters and correlation coefficients for the studied situations are listed in Table 5.

The degree of fitting of the models to the experimental data, given by the correlation coefficient, show that the kinetics of paraquat adsorption is well represented by both models, with correlation factors higher than 0.99 in all cases.

Due to the molecular structure of paraquat, the negatively charged surface of the clay adsorbent and the fast decrease in residual paraquat concentration at a short time scale that suggests a strong electrostatic interaction between the sorbent and paraquat molecules, pseudo-second order model is usually applied [129, 165]. However, it seems that in the studied situations, a pseudo-first order model is also a good option to fit the experimental data and describe the adsorption process.

The rate constants obtained by fitting the pseudo-second order model are significantly high when compared with the literature [165, 181].

Table 5: Kinetic parameters and correlation coefficient (R^2) for paraquat adsorption onto kaolin and mixed suspensions exposed to a 50 mg L^{-1} solution of paraquat (23 ºC, 440 rpm, pH 6 and 30 min of contact time). The kinetic parameters presented in this table are the amount of solute adsorbed at equilibrium (q_e), the rate constant of pseudo-first order sorption model (k_1) and the rate constant of pseudo-second order sorption model (k_2).

Adsorbent	Adsorbent dosage ($g\ L^{-1}$)	Kinetic coefficients					
		Pseudo first order model			Pseudo second order model		
		q_e ($mg\ g^{-1}$)	k_1 (min^{-1})	R^2	q_e ($mg\ g^{-1}$)	k_2 ($g\ mg^{-1}\ min^{-1}$)	R^2
Kaolin	2	6.544 ± 0.049	1.997 ± 0.211	0.997	6.602 ± 0.090	1.110 ± 0.398	0.993
Kaolin + Hematite	2+1	3.626 ± 0.020	2.469 ± 0.224	0.999	3.652 ± 0.020	3.018 ± 0.631	0.998

4.2.1.2. Mass transfer coefficients

As previously mentioned, mass transfer coefficients assess the rate at which equilibrium is approached which may control the time required for a given separation to occur [156]. As such, it is very important to consider this parameter in sorption processes.

Through the use of the Boon-Long correlation [157], mass transfer coefficients were determined for the transport of paraquat onto kaolin (2 g L^{-1}) and kaolin/hematite mixture ($P_{K/IO}$= 2:1) in agitated vessels with a stirring speed of 440 rpm. The obtained values of mass transfer coefficient were 1.10 × 10^{-4} and 1.23 × 10^{-4} m s^{-1} for kaolin and mixed particle suspensions, respectively.

Addicionally, in order to establish a comparison between the order of magnitude of mass transfer coefficients and pseudo-first order rate constants (k_1), a conversion of units was necessary. With this intent, the pseudo first-order adsorption rate constant was converted to 's^{-1}' units and multiplied by the ratio between the liquid volume and sorbent area - $k_1 \times (V_L/A)$ - resulting in values of 1.21 × 10^{-6} and 1.12 × 10^{-6} m s^{-1} for kaolin and mixed particles, respectively. Establishing now the comparison previously mentioned, it can be seen that the adsorption rate constant is two order of magnitude below the mass transfer coefficient in the same experiments, 1.1 x 10^{-4} and 1.23 × 10^{-4} m.s^{-1}, respectively. This indicates that external mass transfer may not be controlling these situations. When the value of the coefficient is comparatively high, mass transfer is fast, equilibrium is reached in seconds or minutes [182] and the overall process

rate depends mainly on the rate at which the interactions occur in the sorbent.

4.2.2. Factors affecting sorption of paraquat onto suspended particles

A sorption process may be affected by factors inherent to the adsorbent itself such as grain-size distribution, specific surface area or mineral constituents [57], by the physico-chemical environment of the adsorption system, such pH, salinity or temperature [129] and also by the chemical characteristics of the solute.

Under this topic, some factors were tested in order to assess their effects on paraquat adsorption process onto kaolin and mixed particle (kaolin/hematite) suspensions.

4.2.2.1. Sorbent concentration effect in paraquat adsorption onto suspended particles

According to the data presented in Figures 9 and 10, the higher the concentration of sorbent, the less residual paraquat remained in the bulk solution. This translates the adsorption capacity of the sorbent for a given

concentration of chemical. Considering the same initial quantity of chemical, the increase in the adsorbent dosage leads to an improvement in the removal efficiency leading to a greater amount of adsorbed chemical, as expected.

Relating the data from this assay to the ones from the standard adsorption studies (section 4.2.1.), it seems that the amount of adsorbent does not affect the adsorption rate, i.e. equilibrium is still achieved very rapidly, only the amount of bounded paraquat in the equilibrium being affected. This conclusion supports the assumption that, from the moment paraquat contacts with the sorbent, interaction occurs, immediately promoting the neutralization of the charges in the mineral particles and quickly leading to an equilibrium state, as previously referred to.

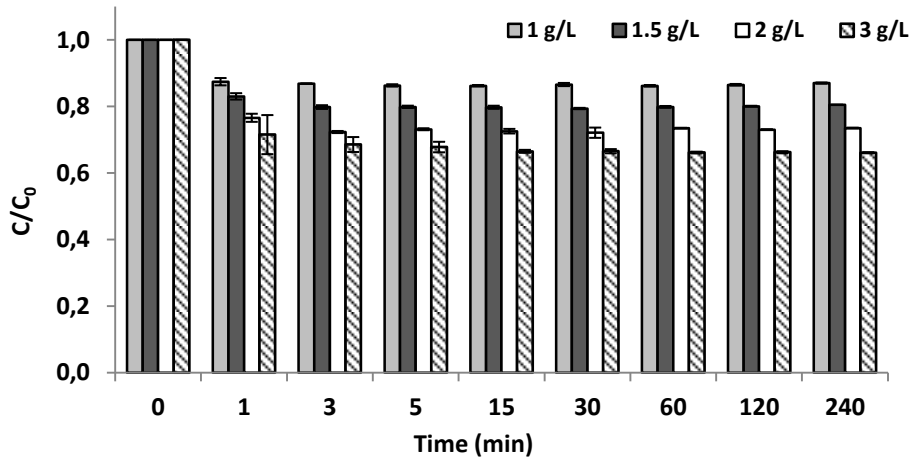

Figure 9: Changes in paraquat concentration overtime, using different dosages of kaolin suspensions (1, 1.5, 2 and 3 g L^{-1}) exposed to a 50 mg L^{-1} paraquat solution (23 ºC, 440 rpm, pH 6). Means with standard deviation determined for two replicates are illustrated.

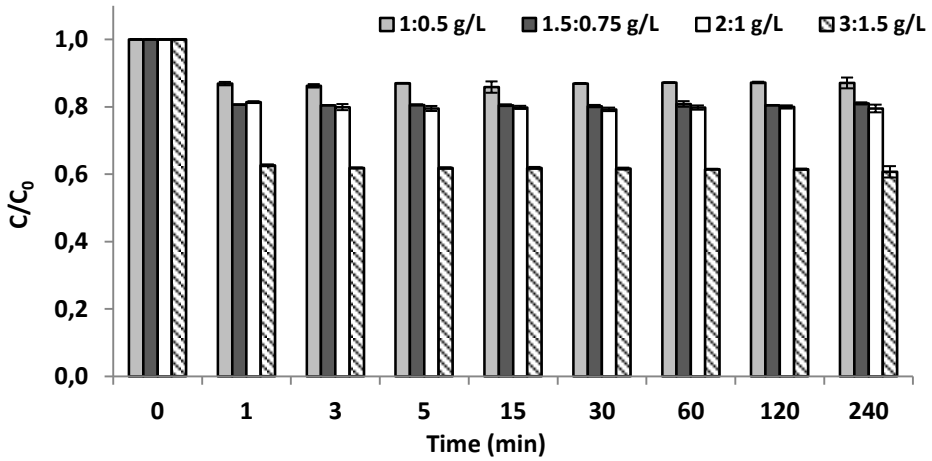

Figure 10: Changes in paraquat concentration overtime, using different dosages of a mixture of kaolin and hematite suspensions, $P_{K/IO}$= 2:1 (1+0.5, 1.5+0.75, 2+1 and 3+1.5 g L^{-1}) exposed to a 50 mg L^{-1} paraquat solution (23 ºC, 440 rpm, pH 6). Means with standard deviation determined for two replicates are illustrated.

To better understand and analyse the effect of adsorbent dosage, kinetic parameters were determined (Table 6).

It is clear that for all the systems in this study the kinetics of paraquat adsorption is truthfully adjusted by the two sorption models, presenting regression coefficients above 0.9.

It also should be noted that the kinetic parameters are presented as a function of adsorbent mass and so, as expected, paraquat concentrations in the sorbent at the equilibrium for the different situations are very similar within each study.

For some situations (lower dosages of kaolin/hematite suspensions) it was not possible to determine the kinetic coefficients due to the lack of adsorbed quantity values between q (t = 0) and q ($t = t_{equilibrium}$).

Table 6: Kinetic parameters and correlation coefficient (R^2) for paraquat adsorption onto different dosages of kaolin and mixed suspensions exposed to a 50 mg L^{-1} solution of paraquat (23 ºC, 440 rpm, pH 6 and 240 min of contact time). The kinetic parameters presented in this table are the amount of solute adsorbed at equilibrium (q_e), the rate constant of pseudo-first order sorption model (k_1) and the rate constant of pseudo-second order sorption model (k_2).

Adsorbent	Adsorbent dosage ($g\ L^{-1}$)	Kinetic coefficients					
		Pseudo first order model			Pseudo second order model		
		q_e ($mg\ g^{-1}$)	k_1 (min^{-1})	R^2	q_e ($mg\ g^{-1}$)	k_2 ($g\ mg^{-1}\ min^{-1}$)	R^2
Kaolin	1	7.494 ± 0.060	2.644 ± 0.299	0.995	7.545 ± 0.070	1.676 ± 0.600	0.996
	1.5	6.470 ± 0.040	1.860 ± 0.101	0.998	6.543 ± 0.079	0.928 ± 0.210	0.993
	2	6.544 ± 0.050	1.997 ± 0.211	0.997	6.602± 0.088	1.110 ± 0.398	0.993
	3	5.915 ± 0.060	1.928 ± 0.199	0.995	6.020 ± 0.020	0.854 ± 0.040	1.000
Kaolin + Hematite	2;1	3.626 ± 0.021	2.469 ± 0.224	0.999	3.652 ± 0.020	3.018 ± 0.631	0.998
	3;1.5	4.085 ± 0.020	3.558 ± 0.401	0.999	4.100 ± 0.010	7.058 ± 1.999	0.999

4.2.2.2. Agitation speed effect in paraquat adsorption onto suspended particles

The effect of agitation speed on paraquat adsorption using adsorbent dosages of 2 g L^{-1} of kaolin and a mixture of 2 g L^{-1} of kaolin plus 1 g L^{-1} of hematite with an initial paraquat concentration of 50 mg L^{-1} is shown in Figure 11. This assay was carried out using two different agitations speeds (330 and 550 rpm) and the collected data suggest that variations in this parameter seem to have a negligible effect on paraquat adsorption onto the suspended particles. This result is supported by the study of Tsai *et al.* [129] for the adsorption of paraquat onto activated clay, were the effect of agitation speed ranging from 200 to 600 rpm on paraquat adsorption was also considered insignificant.

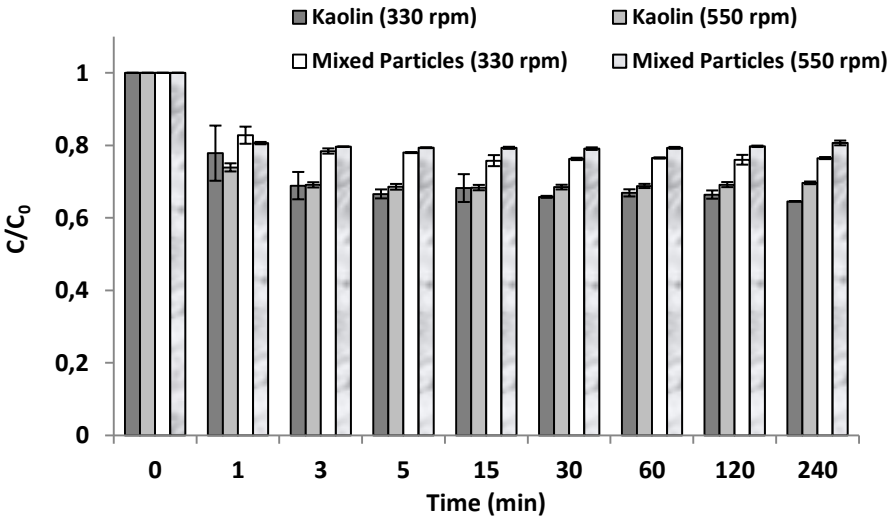

Figure 11: Variations in paraquat concentration overtime for kaolin (2 g L^{-1}) and mixed particle ($P_{K/IO}$= 2:1) suspensions exposed to a 50 mg L^{-1} paraquat solution at different agitation speeds (330 and 550 rpm, 23 ºC, pH 6). Means with standard deviation determined for two replicates are illustrated.

The kinetic parameters k_1 and k_2, in Table 7 rise with the increase in the agitation speed, although the order of magnitude is the same for both stirring situations. This is in disagreement with the comparative analysis of the mass transfer and kinetic parameters presented above (section 4.2.1.2.). One possible explanation is that the higher stirring speeds produce higher shear stresses close to the particles which may reduce the degree of aggregation of kaolin plates and, as such, increase the mass transfer area available for adsorption. Additionally, it should be emphasized that the scarce amount of data between t=0 and t= $t_{equilibrium,}$ may also bring inaccuracies to the application of the kinetic models in this particular situation.

Table 7: Kinetic parameters and correlation coefficient for paraquat adsorption onto kaolin and mixed suspensions exposed to a 50 mg L^{-1} solution of paraquat and tested with different agitation speeds (23 ºC, pH 6 and 240 min of contact time). The kinetic parameters presented in this table are the amount of solute adsorbed at equilibrium (q_e), the rate constant of pseudo-first order sorption model (k_1) and the rate constant of pseudo-second order sorption model (k_2).

Adsorbent	Agitation speed (rpm)	Kinetic coefficients					
		Pseudo first order model			Pseudo second order model		
		q_e (mg g^{-1})	k_1 (min^{-1})	R^2	q_e (mg g^{-1})	k_2 (g mg^{-1} min^{-1})	R^2
Kaolin	330	6.026 ± 0.101	1.428 ± 0.211	0.982	6.217 ± 0.121	0.398 ± 0.060	0.986
	550	5.805 ± 0.060	2.217 ± 0.096	0.994	5.918 ± 0.070	0.813 ± 0.100	0.994
Kaolin + Hematite	330	4.219 ± 0.060	1.442 ± 0.110	0.988	4.365 ± 0.031	0.549 ± 0.039	0.997
	550	3.821 ± 0.032	2.925 ± 0.200	0.996	3.870 ± 0.060	2.040 ± 0.500	0.988

4.2.2.3. Initial pH effect on paraquat adsorption into kaolin particles

The solution's pH is an important variable in adsorption processes. The effect of this parameter was evaluated using two different pH values (3 and 7).

The results obtained from this study (Figure 12) show that the adsorption behaviour within acidic and neutral conditions is similar. Equilibrium is achieved almost instantly implying that pH variations do not have a meaningful effect ($P>0.05$) on paraquat adsorption onto kaolin. An alkaline medium was also tested; however, due to analytical limitations, no valid data was collected.

Comparing these results with some others reported in the literature, Rytwo *et al.* [183], in their study on diquat, paraquat and methyl green adsorption on sepiolite, indicated that adsorption of paraquat was essentially independent of pH in the range of 4.5–8.5; Tsai *et al.* [184], in their study on paraquat adsorption onto activated bleaching earth referred that at pH ranges of 3-8, the effect of this parameter could be considered negligible; Draoui *et al.* [174], in their study on paraquat adsorption onto minerals, indicate that using kaolinite, maximum amount of adsorbed paraquat is pH-dependent, increasing with the rise of pH values; studies performed by Tsai and other authors [129], regarding paraquat adsorption on regenerated clay mineral [11] and activated clay [60, 129] reported that as the pH increased, the adsorbed amount of cationic paraquat increased in response, i.e. paraquat adsorption in these adsorbents is pH-dependent.

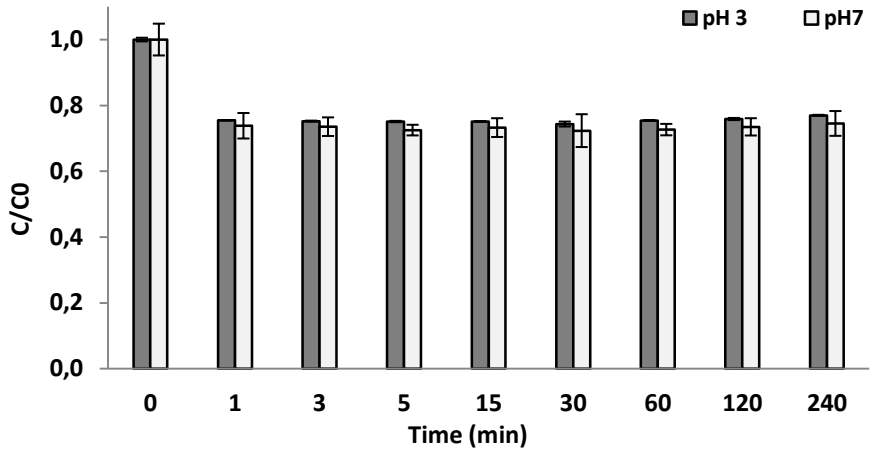

Figure 12: Variations in the paraquat concentration remaining in the bulk solution overtime for a 2 g L^{-1} dosage of kaolin suspension exposed to a 50 mg L^{-1} paraquat solution (23 ºC, 440 rpm, pH 6), using two different values of initial pH, 3 and 7. Means with standard deviation determined for two replicates are illustrated.

The available information does not offer a strike tendency regarding what would be expected about the effect of pH in paraquat adsorption onto clays. Considering the results reported by Draoui *et al.* [174], it would be expected that paraquat adsorption onto kaolin would be directly related to pH increments; however, in this study this was not verified.

Data from the performed studies were analysed by using the pseudo-first and pseudo-second order models. The kinetic parameters values obtained are listed in Table 8.

By analysing this data it can be seen that both situations are well adjusted by the chosen sorption models, presenting correlation coefficients above 0.99.

In terms of kinetic parameters, the experiments performed at different pH, endorse that, in these conditions, this parameter does not have any significant influence on the adsorption process.

Table 8: Kinetic parameters and correlation coefficient for paraquat adsorption onto kaolin suspensions (2 g L^{-1})exposed to a 50 mg L^{-1} solution of paraquat and tested with two different pH values (3 and 7, 23 ºC, 440 rpm and 240 minutes of contact time). The kinetic parameters presented in this table are the amount of solute adsorbed at equilibrium (q_e), the rate constant of pseudo-first order sorption model (k_1) and the rate constant of pseudo-second order sorption model (k_2).

Adsorbent	pH	Kinetic coefficients					
		Pseudo first order model			Pseudo second order model		
		q_e (mg g^{-1})	k_1 (min^{-1})	R^2	q_e (mg g^{-1})	k_2 (g mg^{-1} min^{-1})	R^2
Kaolin	3	6.173 ± 0.070	2.421 ± 0.387	0.992	6.202 ± 0.091	1.997 ± 0.197	0.995
	7	6.080 ± 0.060	2.678 ± 0.401	0.995	6.110 ± 0.070	2.421 ± 0.270	0.997

4.2.3. Paraquat adsorption isotherm studies

From the data presented in Figure 13, the differences between the sorption behaviour among the different types of adsorbents are clear. The adsorption capacity values of hematite are considerably low, compared to the remaining cases. On the other hand, the maximum adsorption capacity of the kaolin/hematite mixture is lower than the one obtained using only kaolin. This is in agreement with the information obtained from the kinetic parameters determined for the adsorption studies. This result could indicate an inhibitory effect promoted by the presence of hematite particles that was not registered in the adsorption studies, possibly due to the fact that paraquat concentration used in the adsorption assays (50 mg L^{-1}) is relatively smaller than the maximum concentration used in the isotherm studies (100 mg L^{-1}). Taking into account the isotherm curves, the point corresponding to an initial concentration of paraquat of 50 mg L^{-1} is the last point where the curves overlap.

Analysing the isotherm curvature, it is known that a downward curvature indicates a favourable isotherm and that an upward curvature points towards an unfavourable isotherm [139]. The studies performed with kaolin and kaolin/hematite mixture fit into the first category whereas the studies performed with hematite can be inserted in the second. This is in agreement with the data collected from the adsorption assays, where hematite effect on the adsorption was not related with the amount of adsorbed chemical. Furthermore an isotherm that is strongly favourable for adsorption, as the case of kaolin and mixed suspensions will be strongly

unfavourable for the recovery of adsorbed species [139]. This finding helps to explain the desorption results.

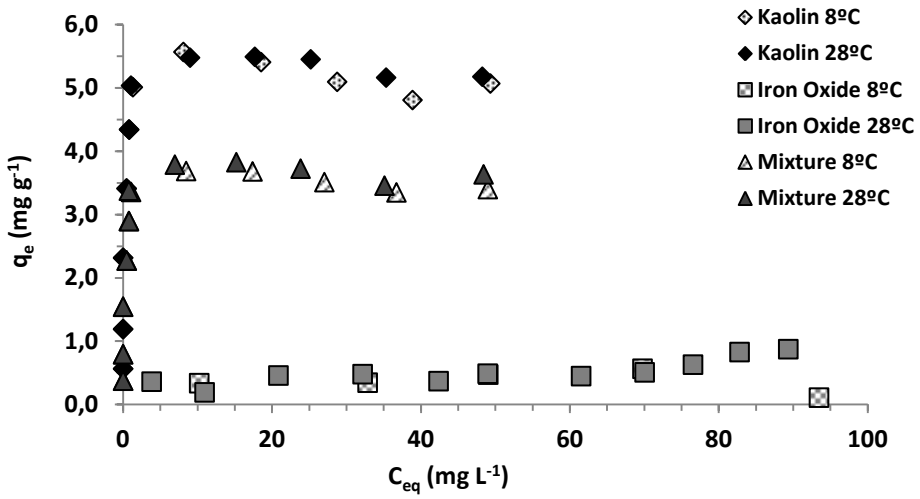

Figure 13: Effect of adsorbent composition (kaolin (10 g L^{-1}); hematite (5 g L^{-1}) or kaolin/hematite ($P_{K/IO}$= 2:1)) and temperature (8 and 28ºC) in paraquat adsorption isotherms (initial paraquat concentrations between 5 and 100 mg L^{-1}, 150 rpm, pH 6 240 min of contact time).

Another important aspect to consider is the shape of adsorption isotherms because it provides information about the adsorption mechanisms. According to Giles *et al.* [185], isotherms can be classified into several categories (Figure 14) based on the initial slope which depends on the rate of site availability changes.

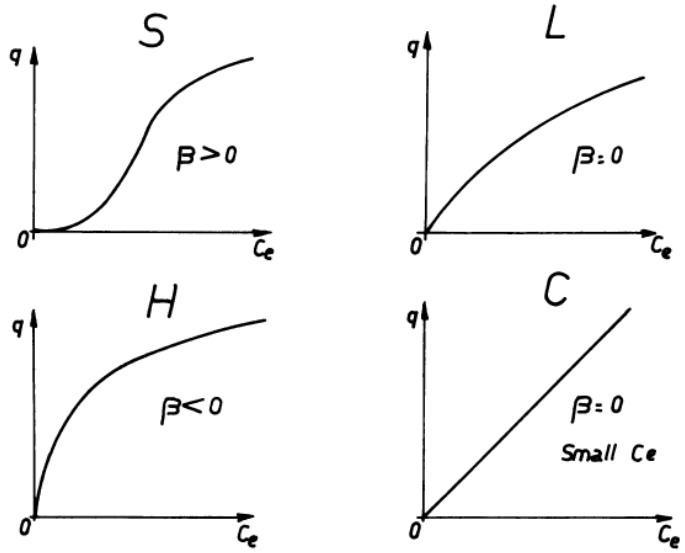

Figure 14: Different shapes of adsorption isotherms. In these illustrations **q** is the amount of solute adsorbed and $\mathbf{C_e}$ is the equilibrium concentration [186].

S-ISOTHERMS: In this type of isotherm, adsorption becomes easier as the concentration in the liquid phase increases [186]. This situation occurs when the solute molecule is attracted to the sorbent, leading to a vertical packing in the adsorbed layer, and encounters a strong competition for sites from molecules of solvent or of another species [185].

L-ISOTHERMS: In this kind of isotherm, there is a decrease of site availability as the solution concentration increases. This means that molecules are probably being adsorbed in a flat position and also that there is not a strong competition from solvent molecules [185].

H-ISOTHERMS: This type of isotherm is a special case of L- isotherms. It occurs when there is a high affinity between the adsorbent surface and the adsorbed solute [186].

C-ISOTHERMS: This type of isotherm takes place when there is a constant partition of the solute between the bulk solution and the adsorbent [185]. Some examples of conditions that favour the occurrence of these isotherms are the existence of a porous substrate with flexible molecules and regions with different degrees of solubility for the solute and solutes with higher affinity for the substrate than for the solvent [186].

Focusing the analysis on the shape of the experimental paraquat adsorption isotherms obtained with kaolin and mixed suspensions, they may be classified as H-type in the Giles classification. As previously mentioned, this class of isotherms occur when the adsorbent possesses a high affinity for the adsorbed solute [186]. According to this, the adsorption behaviour can be explained by the high affinity of the kaolin particles for paraquat. In many cases, this affinity translated in a paraquat removal close to 100%, particularly for the lowest concentrations. This affinity then decreases as the chemical concentration increases because the adsorption of additional molecules becomes more difficult due to the progressive lack of specific sites and/or to the presence of less attractive sites. The increase of chemical concentration leads to a saturation of the sorbent surface.

Regarding the effect of temperature on the maximum adsorption capacity, none of the studied situations appeared to indicate sensitivity to this factor in the studied temperature range.

4.2.3.1. Isotherm parameters

The parameters of adsorption isotherms are compiled in Table 9 and in general, both models (Langmuir and Freundlich) fit the experimental data quite well; however, the Langmuir isotherm presents slightly higher correlation coefficients and slightly smaller normalized standard deviation, which make it a better approach for the equilibrium data experimentally obtained.

In several studies, Freundlich model is normally pointed as a better fit, presenting the highest values of R^2 [60, 165, 181]. This may be related to the experimental conditions, because both models present a very similar adjustment for the obtained results (Figure 15).

Regarding the effect of temperature, it can be seen that the studied situations appeared to be unaffected by this factor in the range of temperatures considered.

Table 9: Adsorption isotherm parameters, correlation coefficient ($R^{"}$) and normalized standard deviation (SD) (kaolin (10 g L^{-1})and kaolin/hematite ($P_{K/IO}$= 2:1) mixture, initial paraquat concentrations between 5 and 100 mg L^{-1}, 8 and 28ºC, 150rpm and 240 minutes of contact time). The isotherm parameters presented in this table are the maximum adsorption capacity of the adsorbent (q_{max}), the Freundlich isotherm constant (n_F), the adsorption equilibrium constant of Langmuir isotherm (K_F) and the adsorption equilibrium constant of Langmuir isotherm (K_L).

Temperature (ºC)	Sorbent Type	Langmuir Isotherm				Freundlich Isotherm			
		q_{max} (mg g^{-1})	K_L (L mg^{-1})	R^2	SD (%)	n	K_F (mg g^{-1}(mg L^{-1})$^{-1/n}$)	R^2	SD (%)
28	Kaolin	5.447±0.396	4.713±3.201	0.928	9.7	16.75±11.90	4.402±0.500	0.901	10.5
	Mixture	3.746±0.310	4.739±3.011	0.922	10.0	15.98±10.60	3.003±0.301	0.895	10.7
8	Kaolin	5.277±0.400	5.202±3.899	0.919	9.9	20.20±17.71	4.387±0.510	0.887	10.6
	Mixture	3.588±0.302	4.929±3.476	0.921	10.0	18.48±14.60	2.943±0.299	0.892	10.6

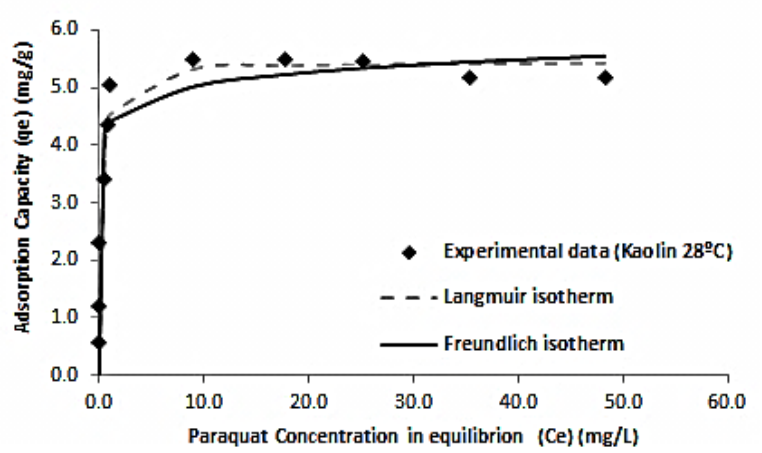
Adsorption Capacity (qe) (mg/g)
6.0
5.0
4.0
3.0
2.0
1.0
0.0
0.0
10.0
20.0
30.0
40.0
50.0
60.0
Paraquat Concentration in equilibrion (Ce) (mg/L)
Experimental data (Kaolin 28ºC)
Langmuir isotherm
Freundlich isotherm

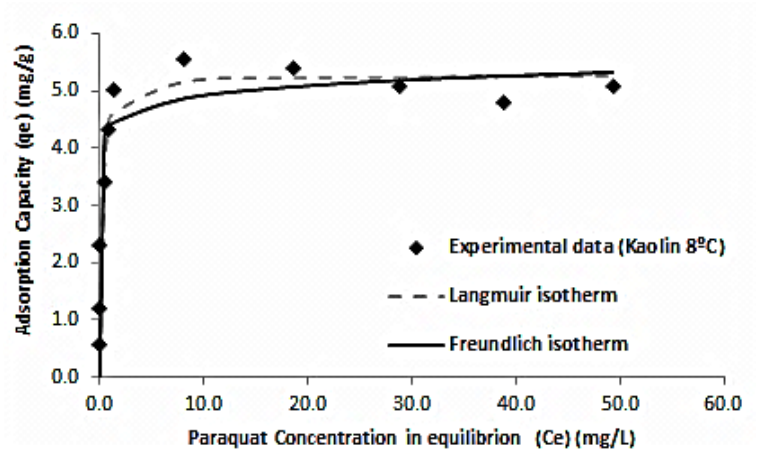
Adsorption Capacity (qe) (mg/g)
6.0
5.0
4.0
3.0
2.0
1.0
0.0
0.0
10.0
20.0
30.0
40.0
50.0
60.0
Paraquat Concentration in equilibrion (Ce) (mg/L)
Experimental data (Kaolin 8ºC)
Langmuir isotherm
Freundlich isotherm

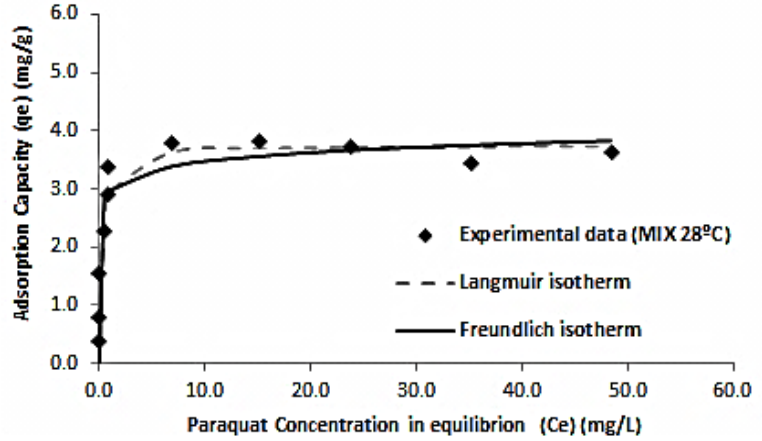
Adsorption Capacity (qe) (mg/g)
6.0
5.0
4.0
3.0
2.0
1.0
0.0
0.0
10.0
20.0
30.0
40.0
50.0
60.0
Paraquat Concentration in equilibrion (Ce) (mg/L)
Experimental data (MIX 28ºC)
Langmuir isotherm
Freundlich isotherm

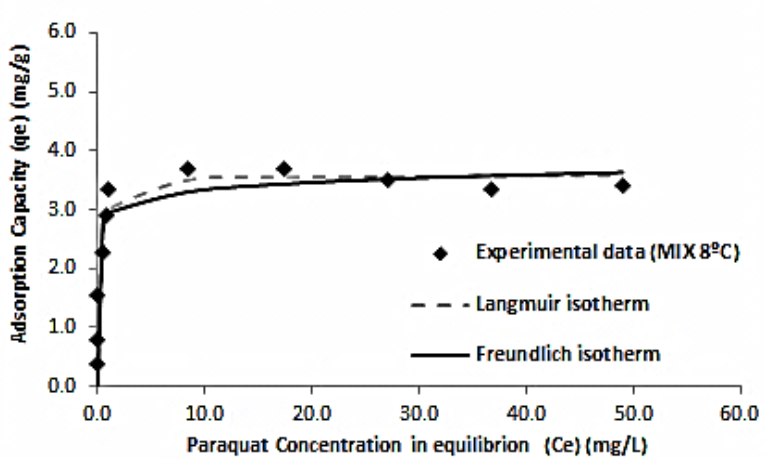

Figure 15: Adsorption isotherms (kaolin and kaolin/hematite mixture, 8 and 28 ºC, 150 rpm and contact time of 240 minutes).

4.2.4. Characterization of adhered deposits formed using kaolin and mixed particle suspensions

Adhered deposits were formed using suspensions of kaolin (2 g L^{-1}) and kaolin/hematite mixture ($P_{K/IO}$= 2:1) that were left re-circulating in a flow cell set up, for a period of twenty and ten days, respectively. After deposit formation, representative samples, collected from different areas in the flow cell, were analysed so that adhered deposits could be characterized in terms of thickness, wet and dry mass. The collected data is presented in Table 10.

Table 10: Different parameters used to characterize deposits of kaolin and kaolin/hematite mixture, formed in the flow cell apparatus.

Type of deposit	Properties		
	Wet Weight (g)	Dry Weight (g)	Thickness (mm)
Kaolin	0.20 ± 0.05	0.010 ± 0.005	0.4 ± 0.2
Kaolin + hematite	0.30 ± 0.03	0.02 ± 0.01	0.7 ± 0.3

Comparing the different parameters for the two types of deposits, it is clear that mixed deposits exhibit higher values, most likely due to the structural combination of iron (III) oxide and kaolin particles. As will be discussed further below, during mixed deposits formation, spherical particles of iron oxide get lodged between kaolin plates preventing its complete aggregation. This promotes a higher thickness in mixed deposits and probably causes an accumulation of total particles on the coupons surface, increasing wet and dry masses.

4.2.5. Adsorption of paraquat onto adhered deposits

In this research study the concept of deposit as an adhered set of particles onto a surface was tested in terms of sorption kinetics modeling. No published results were found on the interaction between paraquat (or similar compounds) and attached deposits.

Initially, paraquat adsorption on adhered deposits of kaolin and kaolin/hematite mixture was studied using the flow cell device; however,

this methodology proved to be ineffective. The reasons why the coupons had to be removed from the flow cell and exposed to paraquat in the small wells of the microplate were:

1.) It proved to be impossible to quantify the decrease in paraquat concentration (caused by adsorption on deposits) in the flow cell circulating solution due to the large volume of liquid compared with the small amount of deposit;

2.) It was also not possible to quantify the amount of paraquat adsorbed into the deposit, because attempts to desorb the chemical from the solid layers were unsuccessful, as previously mentioned.

By applying the procedure described in section 3.2.8, it was possible to obtain a reduction in residual paraquat of approximately 19% and 72% with kaolin and mixed deposits, respectively (Figure 16).

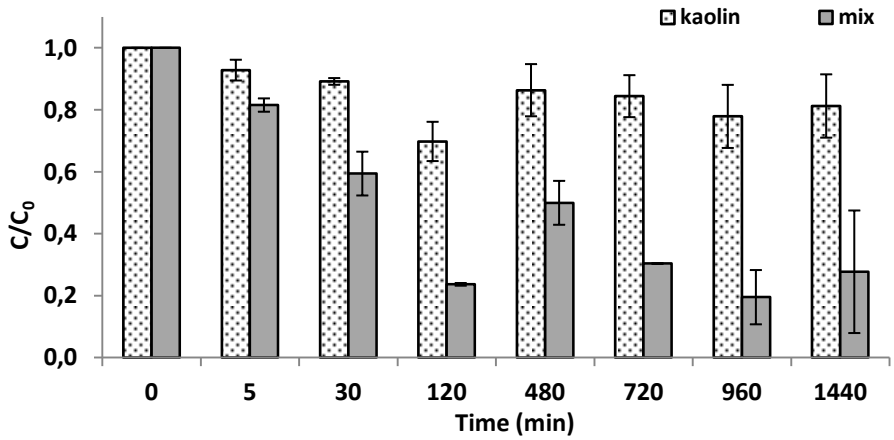

Figure 16: Variations in residual paraquat concentration overtime due to kaolin and kaolin/hematite mixed inorganic deposits exposure to a paraquat solution (50 mg L^{-1}) using the 12 well microplate method (23 ºC and no agitation). Means with standard deviation determined for two replicates are illustrated.

As previously mentioned, models of adsorption diffusion are based on three steps [153]: (1) Diffusion across the liquid surrounding the external surface of adsorbent particles, i.e. external mass transfer; (2) Diffusive migration through the liquid contained in the pores and/or along the pore walls, so called internal diffusion; (3) Adsorption/desorption between the solute and the active sites.

Comparing the results collected from the adsorption assays performed with suspended particles with the ones presented in this section, it is easily seen that with suspended particles the equilibrium is achieved almost instantly while with the adhered deposits the process is much slower. In physical adsorption, interaction with the active sites is a very quick process and can be neglected in kinetic study; the adsorption kinetic process is controlled by internal or external diffusion, i.e. one of the processes should be the rate limiting step [153]. In the case of adhered deposits, the rate limiting step is probably the internal diffusion because of the resistance associated to the deposit porous structure and, enhancing this, there is also the lack of bulk fluid motion which promotes an additional external mass transfer resistance.

Regarding the data obtained for kaolin deposits, relating to the adsorption with suspended particles, even though the mass ratio between sorbent and paraquat is much higher in this situation than with suspended particles, the available area for mass transfer is much smaller due to the face-to-face organization geometry of kaolin particles that results in a very compact deposit (Figure 17).

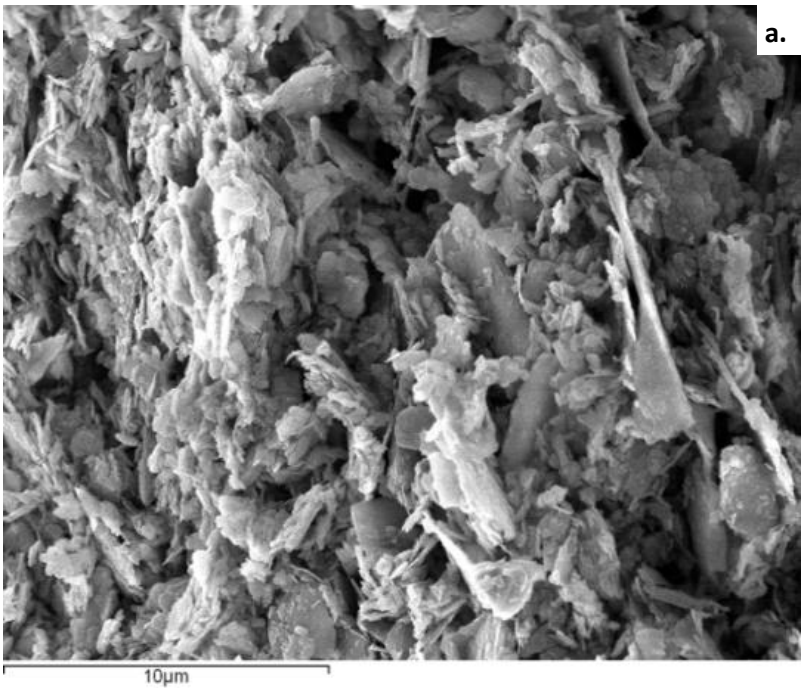
a.
10µm

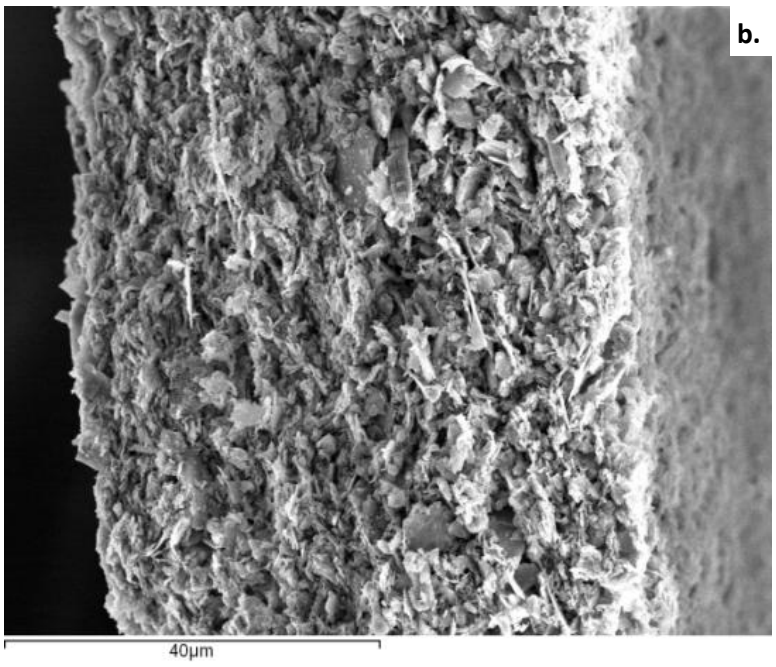
b.
40µm

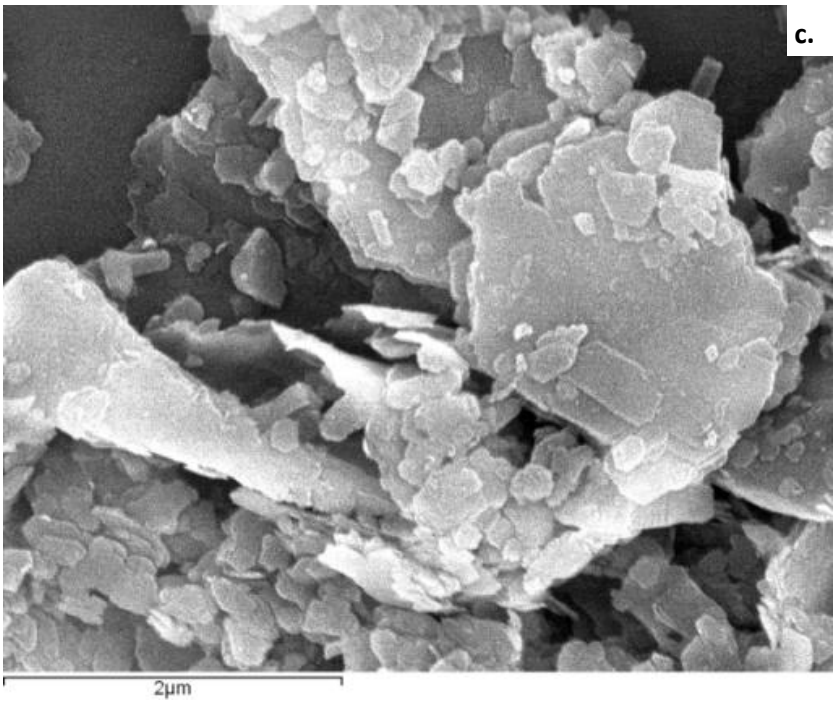

Figure 17: SEM images obtained at CEMUP of the configuration of kaolin deposits: Deposit fracture ((a.) ×1500; (b.) ×5000); Deposit surface ((c.) ×25000)

Analyzing the structural information obtained from SEM images of each deposit (Figure 18), during the formation of mixed deposits, spherical particles of iron oxide become lodged between the kaolin plates (Figure 18b), preventing them from aggregating completely and thereby increasing the mass transfer area of the final deposit. Relating the previous adsorption data with this structural information, the obtained results are consistent and expected.

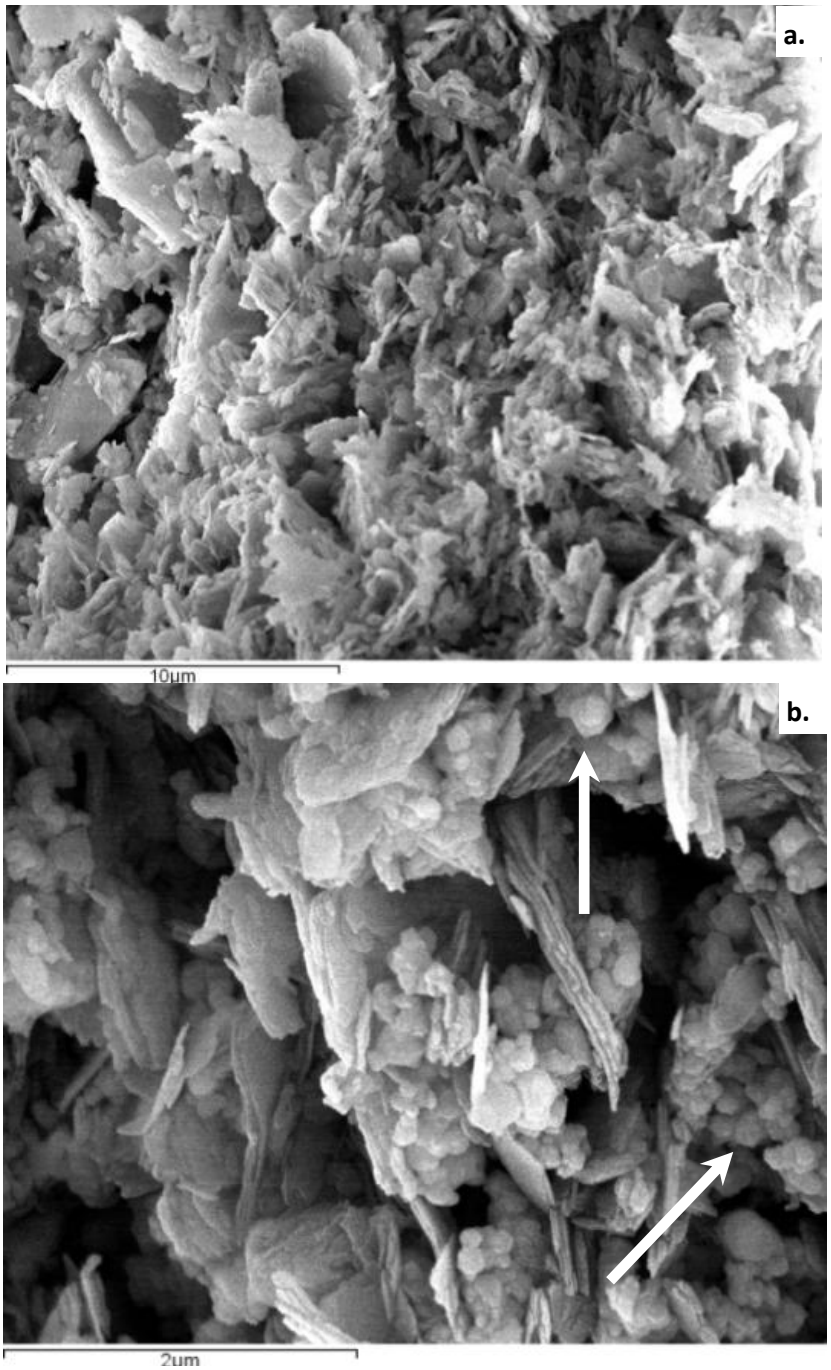

Figure 18: Deposits configuration structures observed with SEM at CEMUP: (a.) Kaolin (×5000); (b.) Kaolin and iron (III) oxide (×25000). Arrows indicate some iron oxide particles inserted between kaolin plates.

4.2.5.1. Kinetic parameters of paraquat adsorption onto inorganic deposits

The values of kinetic parameters and correlation coefficients for the studied situations are listed in Table 11. It is clear that for systems in this study, both adsorption models fit quite well the experimental data, presenting regression coefficients around 0.9.

As previously discussed, there is an important effect of the surface area available for adsorption of chemicals. Suspended particles offer a greater surface than adhered deposit layers for contact with the contaminated water and that explains the much higher rates of adsorption to particles in suspension than to adhered deposits.

Table 11: Kinetic parameters for paraquat adsorption onto kaolin and mixed deposits exposed to a 50 mg L^{-1} paraquat solution (23 ºC, no agitation, pH 6 and 24 hours of contact time). The kinetic parameters presented in this table are the amount of solute adsorbed at equilibrium (q_e), the rate constant of pseudo-first order sorption model (k_1) and the rate constant of pseudo-second order sorption model (k_2).

Adhered Deposit	Ratio (mg sorbent/ mg chemical)	Kinetic coefficients					
		Pseudo first order model			Pseudo second order model		
		q_e (mg g^{-1})	k_1 (min^{-1})	R^2	q_e (mg g^{-1})	k_2 (g mg^{-1} min^{-1})	R^2
Kaolin	**146**	1.064 ± 0.050	0.023 ± 0.007	0.947	1.106 ± 0.080	0.034 ± 0.020	0.917
Kaolin + Hematite	**208**	3.415 ± 0.301	0.010 ± 0.004	0.891	3.852 ± 0.399	0.003 ± 0.002	0.937

4.2.6. Agitation speed effect on paraquat adsorption in adhered deposits

One important limitation of the adsorption studies performed with adhered deposits was that they were carried out without agitation of the bulk solution. Therefore, there was the need to evaluate the effect of agitation on the adsorption process.

Due to the fragility of the deposits produced in the flow cells, deposits of kaolin and mixed particles (kaolin/hematite) were formed in the microplates by sedimentation. The microplates were separated in two groups, the first group was left standing still (static conditions) and the second one was subjected to a constant agitation of 150 rpm in an orbital incubator, as previously described.

The data obtained from these studies are presented in Figure 19 and indicate that, in the presence of agitation, higher adsorption rates are obtained after the first 5 minutes of contact between the chemical and the deposit. During the initial 5 minutes, even though a significant adsorption was already measured (to an extent of 25-30%), the effect of the agitation speed was quite small or negligible. This may be associated to the several stops in agitation (1, 3 and 5 minutes) to collect samples during these initial minutes. The constant interruptions during this short period of time may have affected the efficiency of agitation itself.

Determination of kinetic parameters allowed the quantification of the effect of agitation speed on paraquat adsorption in adhered deposits. Data presented in Table 12 show that adsorption rate constants obtained

with agitation are considerably higher than without it. Comparing the hydrodynamic conditions in stagnant medium and in a perfectly agitated system, mass transfer resistance decreases significantly with agitation allowing a better diffusion of paraquat molecules across the liquid surrounding the external surface of the deposits.

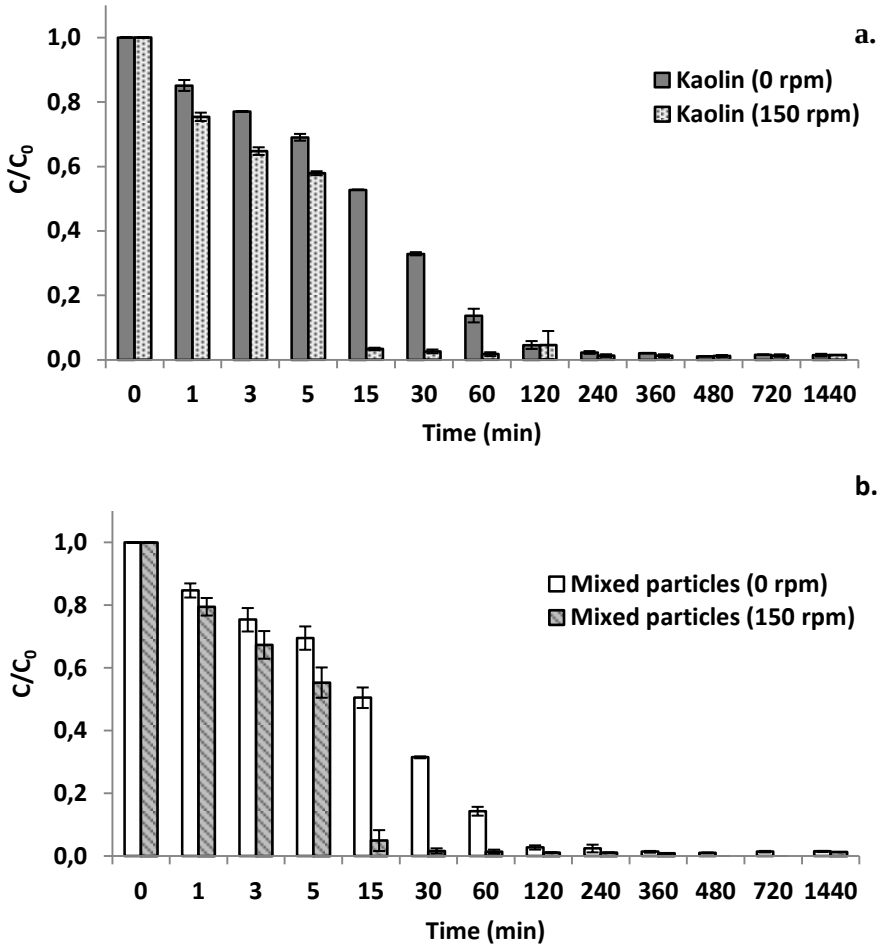

Figure 19: Variations of paraquat concentration overtime during kaolin (10 g L^{-1}) (a.) and kaolin/hematite mixture ($P_{K/IO}$= 2:1 with 10 g L^{-1} of kaolin) (b.) inorganic deposits exposure to a paraquat solution (50 mg L^{-1}) using 12 well microplates (23ºC, 0 and 150 rpm, pH 6 and 24 hours of contact time). Means with standard deviation determined for two replicates are illustrated.

Table 12: Kinetic parameters for paraquat adsorption onto kaolin (10 g L^{-1}) and kaolin/hematite ($P_{K/IO}$= 2:1 with 10 g L^{-1} of kaolin) deposits exposed to a solution of paraquat 50 mg L^{-1} (23 ºC, 0 and 150 rpm, pH 6 and 24 hours of contact time). The kinetic parameters presented in this table are the amount of solute adsorbed at equilibrium (q_e), the rate constant of pseudo-first order sorption model (k_1) and the rate constant of pseudo-second order sorption model (k_2).

Adsorbent	Agitation Speed (rpm)	Kinetic coefficients					
		Pseudo first order model			Pseudo second order model		
		q_e (mg g^{-1})	k_1 (min^{-1})	R^2	q_e (mg g^{-1})	k_2 (g mg^{-1} min^{-1})	R^2
Kaolin	0	5.138 ± 0.100	0.047 ± 0.006	0.986	5.386 ± 0.101	0.014 ± 0.002	0.991
	150	5.239 ± 0.099	0.149 ± 0.020	0.980	5.473 ± 0.199	0.041 ± 0.010	0.955
Kaolin + Hematite	0	3.422± 0.090	0.050 ± 0.006	0.985	3.584 ± 0.060	0.023 ± 0.003	0.991
	150	3.514 ± 0.061	0.143 ± 0.010	0.990	3.679± 0.099	0.058 ± 0.010	0.963

4.3. Preliminary assays performed with chlorfenvinphos

4.3.1. Chlorfenvinphos adsorption onto kaolin suspensions

Applying the methodology described in section 3.3.1, a reduction of approximately 22% in chlorfenvinphos concentration in the bulk solution was obtained under the set conditions.

From the data presented in Figure 20, it is clear that chlorfenvinphos adsorption shows a quick development, stabilizing from the fifth minute of kaolin exposure to the chemical solution, i.e. equilibrium plateau is reached after 5 minutes of interaction.

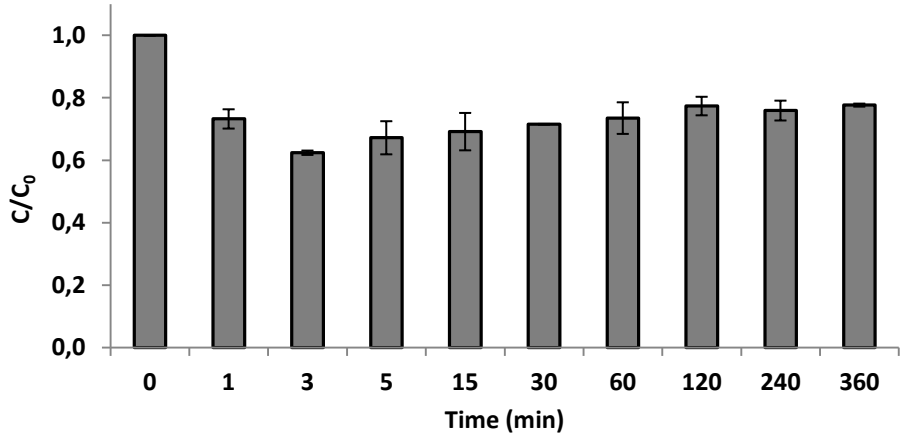

Figure 20: Variations registered in residual chlorfenvinphos concentration overtime due to the exposure of kaolin particles (70 g L^{-1}) to a 10 mg L^{-1} chlorfenvinphos solution. Experiments performed at 550 rpm, 23 ºC and pH 6, during 6 hours. Means with standard deviation determined for two replicates are illustrated.

Published studies regarding the interaction between chlorfenvinphos and clays in general, are scarce, making it difficult to establish a comparative analysis. Garcia *et al.* [135] performed a study on adsorption kinetics of chlorfenvinphos in kaolinite, where adsorption equilibrium was reached after two hours and the maximum amount of chlorfenvinphos adsorbed was 163.3 μg g^{-1}. Comparing with the data obtained in this study, both the maximum amount of chlorfenvinphos adsorbed (1300 μg g^{-1}) and the time needed to achieve equilibrium (5 minutes) were considerably different.

Comparing the experimental procedures, some differences stand out. In the present study, the amount of kaolin used was 3.5 times higher than the concentration of chemical; no thermal treatment was applied to the clay prior to use and the sampling procedure was more direct and less elaborated. In the study presented by Garcia *et al.* [135] the collected samples were initially centrifuged and then an extraction process involving a mixture of petroleum ether/acetone was applied after the addition of a saturated solution of sodium chloride to separate the organic stage. In the experiments here presented, a simple filtration using fibre glass filters was performed on the collected samples.

4.3.2. Agitation speed effect on chlorfenvinphos adsorption onto kaolin particles

To assess the effect of agitation speed on chlorfenvinphos adsorption on kaolin, an adsorbent dosage of 70 g L^{-1} was exposed to a chlorfenvinphos solution with an initial concentration of 10 mg L^{-1} at room temperature (23 ºC) applying three different agitations speeds (330, 550 and 770 rpm). The obtained results are illustrated in Figure 21 which shows that, in general, no significant differences were registered among the different values of agitation speed.

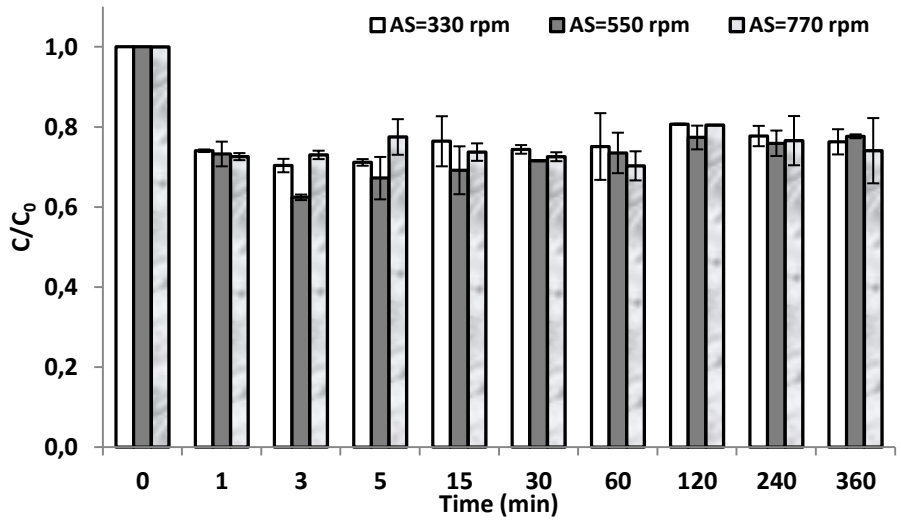

Figure 21: Residual chlorfenvinphos concentration, measured during 6 hours of kaolin particles (70 g L^{-1}) exposure to a 10 mg L^{-1} chlorfenvinphos solution. Experiments performed at 23 ºC and pH 6 using three different agitation speeds (330, 550 and 770 rpm). Means with standard deviation determined for two replicates are illustrated.

These results indicate that, within the range of agitation speeds tested, kaolin particles distribution within the suspensions is homogeneous (not occurring particle sedimentation due to a deficient agitation) and an immediate interaction between the chemical and the active sites in the clay is promoted, i.e. external mass transfer resistance does not seem relevant.

4.3.3. Initial pH effect on chlorfenvinphos adsorption onto kaolin particles

This parameter was evaluated through the exposure of 70 g L^{-1} of adsorbent to a chlorfenvinphos solution with an initial concentration of 10 mg L^{-1} at room temperature (23 ºC) adjusting initial pH to three different values, 3, 7 and 10. The obtained results are illustrated in Figure 22.

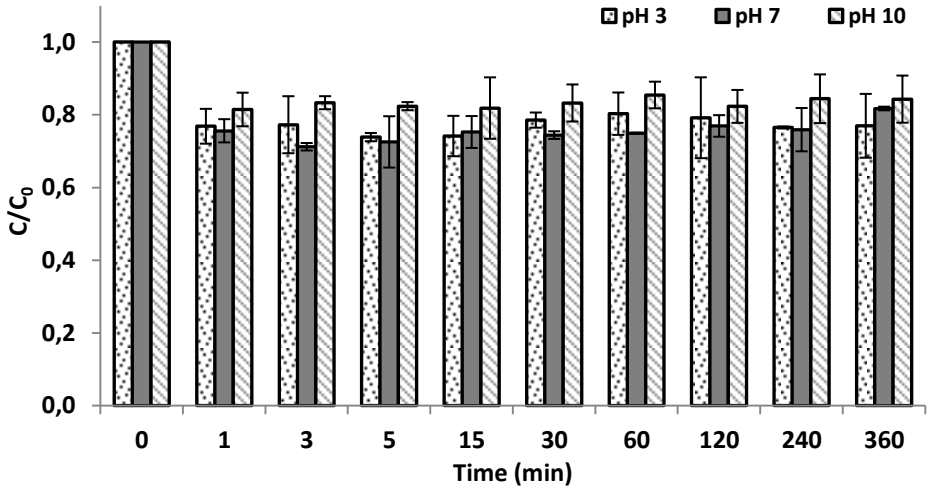

Figure 22: Variations registered in residual chlorfenvinphos concentration overtime due to the exposure of kaolin particles (70 g L^{-1}) to a 10 mg L^{-1} chlorfenvinphos solution. Experiments performed at 550 rpm, 23 ºC, during 6 hours, using three different values of initial pH (3, 7 and 10). Means with standard deviation determined for two replicates are illustrated.

The presented results indicate that, in acidic or neutral medium, the adsorption process is not affected by the pH value of the solution ($P>0.05$). At high pH vales, however, there seems to be a slight negative influence on the amount of chemical adsorbed since the concentration of residual chlorfenvinphos in the bulk is higher than in the other cases.

4.3.4. Temperature effect on chlorfenvinphos adsorption on kaolin particles

This parameter was evaluated through the exposure of 70 g L^{-1} of adsorbent to a chlorfenvinphos solution with an initial concentration of 10 mg L^{-1} at 550 rpm and using three different temperatures 5, 25 and 37 ºC. The obtained results are illustrated in Figure 23.

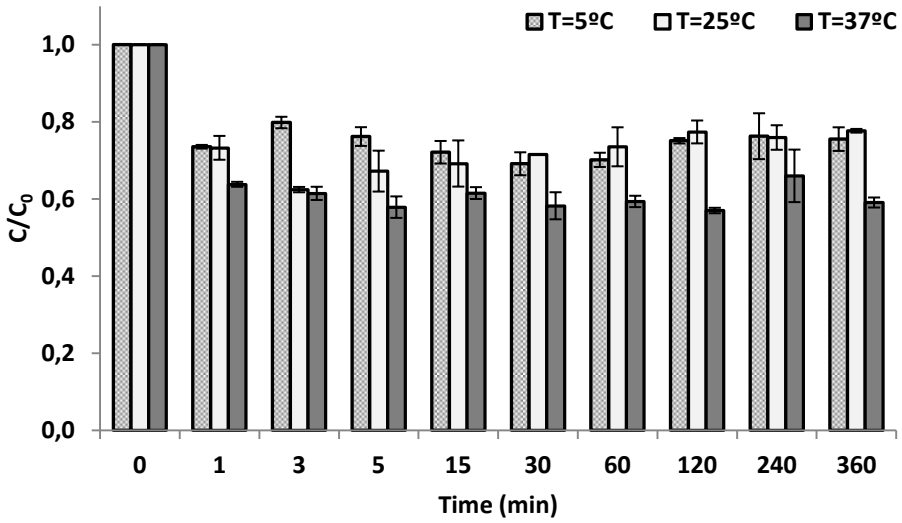

Figure 23: Variations registered in residual chlorfenvinphos concentration overtime due to the exposure of kaolin particles (70 g L^{-1}) to a 10 mg L^{-1} chlorfenvinphos solution. Experiments performed at 550 rpm and pH 6 using three temperatures (5, 25 and 37 ºC), during 6 hours. Means with standard deviation determined for two replicates are illustrated.

The obtained results indicate that higher temperatures seem to favour chlorfenvinphos adsorption onto kaolin particles. Experiments performed at 5 and 25 ºC show a similar behaviour of chlorfenvinphos adsorption ($P>0.05$), leading to the assumption that within this temperature range, temperature does not influence the adsorption process.

4.4. Preliminary assays performed with carbofuran

4.4.1. Carbofuran adsorption onto kaolin and kaolin/hematite mixed suspensions

Applying the methodology described in section 3.4.1, reductions in carbofuran concentration in the bulk solution around 16 and 24 %, respectively with kaolin and kaolin/hematite mixture, were obtained under the set conditions. The adsorption percentage obtained using kaolin is in agreement with some information available in literature. Farahani *et al.* [84] performed a study on carbofuran sorption using sandy clay and clay soil. The percentage of carbofuran adsorption obtained with sandy clay is similar to the one achieved in the present study.

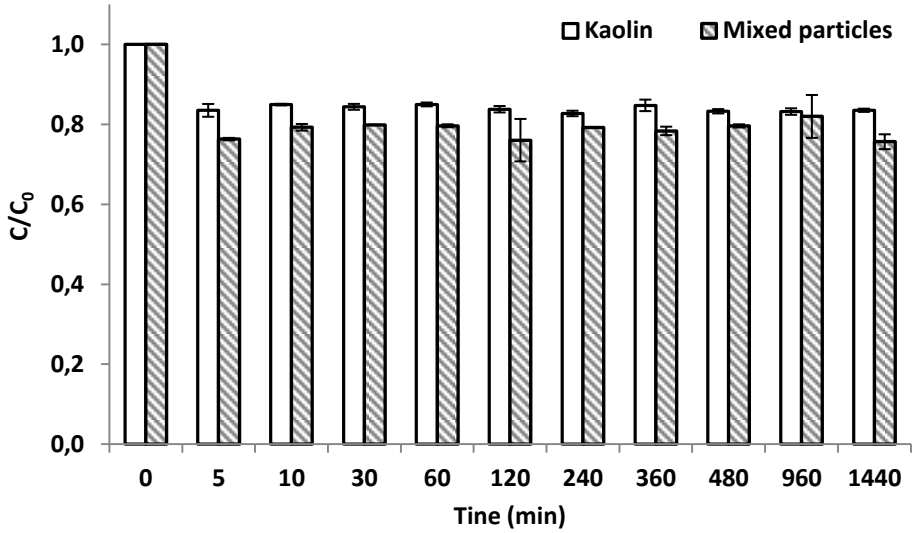

Figure 24: Variations registered in residual carbofuran concentration overtime due to the exposure of kaolin and kaolin/hematite mixture (5g; 5+2.5g, respectively) to a 5 μg g^{-1} carbofuran solution, during 24 hours (23 ºC, 550 rpm and pH 6). Means with standard deviation determined for two replicates are illustrated.

The results shown in Figure 24 indicate that, for both kaolin and mixed kaolin/hematite suspensions, carbofuran adsorption reaches a plateau very rapidly (after 5 and 10 min for kaolin and mixed kaolin/hematite suspensions, respectively). Considering standard deviations and statistical analysis ($P>0.05$), no significant variations where registered in the samples taken overtime. This leads to assume that equilibrium is almost instantaneous.

4.4.2. Initial pH effect on carbofuran adsorption on kaolin particles

To evaluate the influence of this parameter in the adsorption process, 5 g of kaolin (or 5 g of kaolin plus 2.5 g of hematite) was exposed to a carbofuran solution (2.5 mg L^{-1}) at room temperature (23 ºC) adjusting initial pH of the chemical solution to three different values: 3, 7 and 10. The obtained results are illustrated in Figure 25.

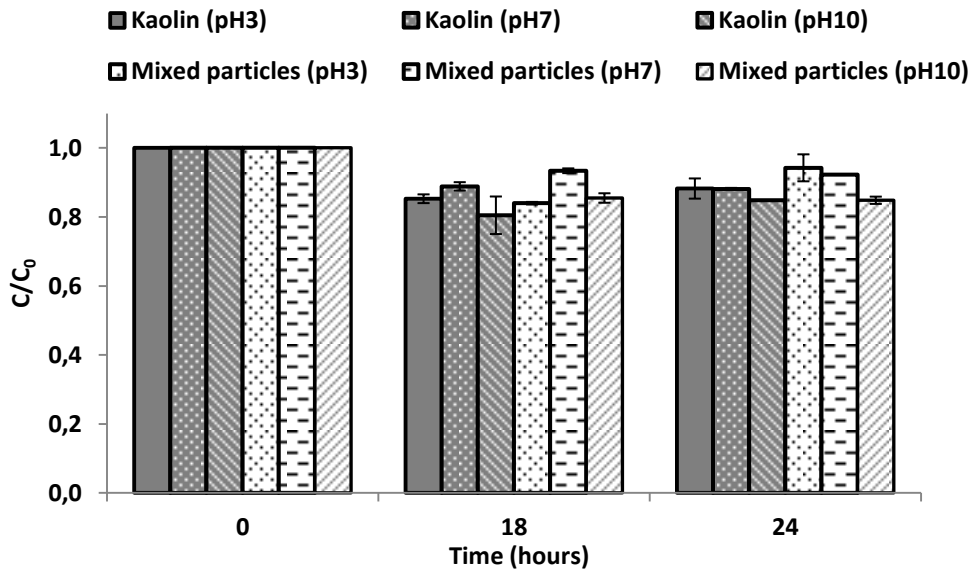

Figure 25: Variations registered in residual carbofuran concentration overtime due to the exposure of kaolin and kaolin/hematite mixture (5g; 5+2.5g, respectively) to a 5 µg g^{-1} carbofuran solution, during 24 hours (23 ºC, 550 rpm). Initial pH of the chemical's solution was adjusted to three different values: 3, 7 and 10. Means with standard deviation determined for two replicates are illustrated.

Analysing the obtained results, an increase in pH value seems to promote a slight enhancement in carbofuran adsorption, while acid and neutral pH values apparently show the same behaviour. In the study developed by Hsieh *et al.* [167], on carbofuran adsorption onto soil samples and in particular in the experiments performed to evaluate pH effect on the adsorption process, using untreated soil, a scenario similar to the one this study is mentioned. The amount of carbofuran adsorbed by the untreated soil was significantly influenced by the pH value. Under low pH conditions, only 2–17% of the amount of carbofuran was adsorbed by soil; however the percentage of carbofuran removal increased up to 50% as the soil pH was raised to a maximum value of 8.5.

Chapter 5.

General Conclusions and Future Work

5.1. General conclusions

The outcome knowledge from this thesis intended to contribute to the development of an appropriate response for rapidly restoring the use of the drinking water network upon a deliberate contamination with pesticides. Specifically, the studies here presented aimed to contribute with kinetic parameters to the modelling of reactive transport in drinking water distribution systems to allow the simulation of contaminants spread throughout the network and the identification of the origin point of the contamination.

This study was mainly focused on paraquat adsorption although some preliminary studies were made on two other chemicals, chlorfenvinphos and carbofuran.

From the studies performed with paraquat, kaolin particles proved to be very good adsorbents, reaching their maximum sorption capacity almost instantaneously and iron (III) oxide presented itself as a facilitator in the adsorption process, promoting an enhancement in the adsorption kinetic constant. It was also shown that the adsorption process was influenced by the adsorbent dosage but not by initial pH or agitation speed, within the tested conditions.

Experiments made with attached deposits revealed that the presence of iron (III) oxide particles within the deposit structure leads to an enhancement in the internal area of the mixed particle deposits improving the adsorption of paraquat.

Determination of kinetic parameters shows that both pseudo-first and pseudo-second order models adjusted experimental data quite well presenting correlation coefficients around 0.99. Comparing the two isotherm models applied, Langmuir's provided a better approach for the adsorption equilibrium results obtained.

The studies performed with chlorfenvinphos and carbofuran allowed the gathering of preliminary information important to better understand these chemicals when in contact with the selected substances. The adsorption of chlorfenvinphos seems to be favored by higher values of temperature and hampered by basic pH values. On the other hand, in the adsorption of carbofuran, a higher pH promotes a more efficient adsorption of this pesticide.

5.2. Suggestions for future work

Much can still be done to evaluate the outcomes of possible contaminations of infrastructures essential for human existence and the development of effective responses, making this a promising research area.

Within the scope of the work developed on this thesis some suggestions for future studies are:

- To optimize the methodology to study pesticide adsorption onto adhered deposits;
- To perform further interaction studies between pesticides and different types of adhered deposits (wider range of inorganic materials, mixture of inorganic and microbiological components);
- To evaluate the interaction of the pesticides used in this study with other components present in the composition of drinking water deposits;
- To deepen the studies performed with carbofuran and chlorfenvinphos;
- To extend these studies to other relevant pesticides;

References

[1] A. Azizullah, M.N.K. Khattak, P. Richter, D.-P. Häder, Water pollution in Pakistan and its impact on public health—a review, Environment International. 37 (2011) 479–497.

[2] R.P. Schwarzenbach, T. Egli, T.B. Hofstetter, U. Von Gunten, B. Wehrli, Global water pollution and human health, Annual Review of Environment and Resources. 35 (2010) 109–136.

[3] N.R.C. (US). C. on L.S.S.D.W. Committee, A. of L.S. (US). S.D.W. Committee, Drinking Water and Health, Volume 1, National Academy Press, 1977.

[4] P.H. Gleick, Water and terrorism, Water Policy. 8 (2006) 481–503.

[5] R. Calderon, The epidemiology of chemical contaminants of drinking water, Food and Chemical Toxicology. 38 (2000) 13–20.

[6] C.M.D. Manuel, Biofilm Dynamics and Drinking Water Stability: Effects of Hydrodynamics and Surface Materials, Faculdade de Engenharia da Universidade do Porto, PhD Thesis, 2007.

[7] H.I. Zeliger, Human Toxicology of Chemical Mixtures: Toxic Consequences Beyond the Impact of One-Component Product and Environmental Exposures, 2nd ed., William Andrew, 2011.

[8] R.T. Delfino, T.S. Ribeiro, J.D. Figueroa-Villar, Organophosphorus compounds as chemical warfare agents: a review, Journal of the Brazilian Chemical Society 20, 3 (2009) 407–428.

[9] R. Gupta, Toxicology of organophosphate & carbamate compounds, Elsevier Academic Press, 2006.

[10] C. Oliveira, M.S. Santos, F. Maldonado-Hódar, G. Schaule, A. Alves, L.M. Madeira, Use of pipe deposits from water networks as novel catalysts in paraquat peroxidation, Chemical Engineering Journal. 210 (2012) 339-349.

[11] W.T. Tsai, C.W. Lai, Adsorption of herbicide paraquat by clay mineral regenerated from spent bleaching earth, Journal of Hazardous Materials. 134 (2006) 144–148.

[12] I. García-Sosa, F.M. Ramírez, Synthesis, Solid and Solution Studies of Paraquat Dichloride Calixarene Complexes. Molecular Modelling, Journal of the Mexican Chemical Society. 54 (2010) 143–152.

[13] F.E. Ahmed, Analysis of pesticides and their metabolites in foods and drinks, Trends in Analytical Chemistry. 20 (2001) 649–661.

[14] P. Rao, R. Mansell, L. Baldwin, M. Laurent, Pesticides and their behavior in soil and water, Institute of Food and Agricultural Sciences - University of Florida. (1983)

[15] T. Ahmad, M. Rafatullah, A. Ghazali, O. Sulaiman, R. Hashim, A. Ahmad, Removal of pesticides from water and wastewater by different adsorbents: A review, Journal of Environmental Science and Health, Part C. 28 (2010) 231–271.

[16] B. Srivastava, V. Jhelum, D.D. Basu, P.K. Patanjali, Adsorbents for pesticide uptake from contaminated water : A review, Journal of Scientific & Industrial Research. 68 (2009).839-850

[17] C. Bolognesi, Genotoxicity of pesticides: a review of human biomonitoring studies, Mutation Research. 543 (2003) 251–272.

[18] G. Lagaly, Pesticide-clay interactions and formulations, Applied Clay Science. 18 (2001) 205–209.

[19] N.K. Hamadi, S. Swaminathan, X.D. Chen, Adsorption of Paraquat dichloride from aqueous solution by activated carbon derived from used tires, Journal of Hazardous Materials. 112 (2004) 133–141.

[20] H. El Bakouri, J. Morillo, J. Usero, A. Ouassini, Natural attenuation of pesticide water contamination by using

ecological adsorbents: Application for chlorinated pesticides included in European Water Framework Directive, Journal of Hydrology. 364 (2009) 175–181.

[21] N. Luque, S. Rubio, Extraction and stability of pesticide multiresidues from natural water on a mixed-mode admicellar sorbent, Journal of Chromatography A. 1248 (2012) 74–83.

[22] R.J. Gilliom, Pesticides in US streams and groundwater, Environmental Science & Technology. 41 (2007) 3408–3414.

[23] M. Cerejeira, P. Viana, S. Batista, T. Pereira, E. Silva, M. Valério, et al., Pesticides in Portuguese surface and ground waters, Water Research. 37 (2003) 1055–1063.

[24] M. Arias-Estévez, E. López-Periago, E. Martínez-Carballo, J. Simal-Gándara, J.-C. Mejuto, L. García-Río, The mobility and degradation of pesticides in soils and the pollution of groundwater resources, Agriculture, Ecosystems & Environment. 123 (2008) 247–260.

[25] M. Liess, P. Ohe, Analyzing effects of pesticides on invertebrate communities in streams, Environmental Toxicology and Chemistry. 24 (2005) 954–965.

[26] F. Geiger, J. Bengtsson, F. Berendse, W.W. Weisser, M. Emmerson, M.B. Morales, Persistent negative effects of pesticides on biodiversity and biological control potential on European farmland, Basic and Applied Ecology. 11 (2010) 97–105.

[27] J.D. Stark, J.E. Banks, Population-level effects of pesticides and other toxicants on arthropods, Annual Review of Entomology. 48 (2003) 505–519.

[28] D. Stajnbaher, L. Zupancic-Kralj, Multiresidue method for determination of 90 pesticides in fresh fruits and vegetables using solid-phase extraction and gas chromatography-mass spectrometry, Journal of Chromatography A. 1015 (2003) 185–198.

[29] C. Lesueur, P. Knittl, M. Gartner, A. Mentler, M. Fuerhacker, Analysis of 140 pesticides from conventional farming foodstuff samples after extraction with the modified QuECheRS method, Food Control. 19 (2008) 906–914.

[30] R.M. Johnson, M.D. Ellis, C.A. Mullin, M. Frazier, Pesticides and honey bee toxicity-USA, Apidologie. 41 (2010) 312–331.

[31] A. Mulchandani, W. Chen, P. Mulchandani, J. Wang, K.R. Rogers, Biosensors for direct determination of organophosphate pesticides, Biosensors and Bioelectronics. 16 (2001) 225–230.

[32] M. Trojanowicz, Determination of pesticides using electrochemical enzymatic biosensors, Electroanalysis. 14 (2002) 1311–1328.

[33] A. Simonian, T. Good, S.-S. Wang, J. Wild, Nanoparticle-based optical biosensors for the direct detection of organophosphate chemical warfare agents and pesticides, Analytica Chimica Acta. 534 (2005) 69–77.

[34] C.C. Leandro, P. Hancock, R.J. Fussell, B.J. Keely, Comparison of ultra-performance liquid chromatography and high-performance liquid chromatography for the determination of priority pesticides in baby foods by tandem quadrupole mass spectrometry, Journal of Chromatography A. 1103 (2006) 94–101.

[35] L. Fu, X. Liu, J. Hu, X. Zhao, H. Wang, X. Wang, Application of dispersive liquid-liquid microextraction for the analysis of triazophos and carbaryl pesticides in water and fruit juice samples, Analytica Chimica Acta. 632 (2009) 289–295.

[36] R. Romero-González, A. Garrido Frenich, J. Martínez Vidal, O. Prestes, S. Grio, Simultaneous determination of pesticides, biopesticides and mycotoxins in organic products applying a quick, easy, cheap, effective, rugged and safe extraction procedure and ultra-high performance liquid chromatography-tandem mass spectrometry, Journal of Chromatography A. 1218 (2011) 1477–1485.

[37] W. Zheng, M. Guo, T. Chow, D.N. Bennett, N. Rajagopalan, Sorption properties of greenwaste biochar for two triazine pesticides, Journal of Hazardous Materials. 181 (2010) 121–126.

[38] S. Malato, J. Blanco, J. Cáceres, A. Fernández-Alba, A. Agüera, A. Rodríguez, Photocatalytic treatment of water-soluble pesticides by photo-Fenton and TiO_2 using solar energy, Catalysis Today. 76 (2002) 209–220.

[39] H. Burrows, M. Canle L, J. Santaballa, S. Steenken, Reaction pathways and mechanisms of photodegradation of pesticides, Journal of Photochemistry and Photobiology B: Biology. 67 (2002) 71–108.

[40] M. Danish, O. Sulaiman, M. Rafatullah, R. Hashim, A. Ahmad, Kinetics for the removal of paraquat dichloride from aqueous solution by activated date (Phoenix dactylifera) stone carbon, Journal of Dispersion Science and Technology. 31 (2010) 248–

259.

[41] R. Meinert, J. Schüz, U. Kaletsch, P. Kaatsch, J. Michaelis, Leukemia and non-Hodgkin's lymphoma in childhood and exposure to pesticides: results of a register-based case-control study in Germany, American Journal of Epidemiology. 151 (2000) 639–646.

[42] S.M. Snedeker, Pesticides and breast cancer risk: a review of DDT, DDE, and dieldrin, Environmental Health Perspectives. 109 (2001) 35-47.

[43] M.C. Alavanja, C. Samanic, M. Dosemeci, J. Lubin, R. Tarone, C.F. Lynch, et al., Use of agricultural pesticides and prostate cancer risk in the Agricultural Health Study cohort, American Journal of Epidemiology. 157 (2003) 800–814.

[44] S.L. Teitelbaum, M.D. Gammon, J.A. Britton, A.I. Neugut, B. Levin, S.D. Stellman, Reported residential pesticide use and breast cancer risk on Long Island, New York, American Journal of Epidemiology. 165 (2007) 643–651.

[45] P.R. Band, Z. Abanto, J. Bert, B. Lang, R. Fang, R.P. Gallagher, et al., Prostate cancer risk and exposure to pesticides in British Columbia farmers, The Prostate. 71 (2011) 168–183.

[46] M.C. Alavanja, M.R. Bonner, Occupational pesticide exposures and cancer risk: a review, Journal of Toxicology and Environmental Health, Part B. 15 (2012) 238–263.

[47] M.C. Alavanja, M.K. Ross, M.R. Bonner, Increased cancer burden among pesticide applicators and others due to pesticide exposure, CA: a Cancer Journal for Clinicians. (2013).

[48] T.P. Brown, P.C. Rumsby, A.C. Capleton, L. Rushton, L.S. Levy, Pesticides and Parkinson's disease—is there a link?, Environmental Health Perspectives. 114 (2006) 156.

[49] J.A. Firestone, T. Smith-Weller, G. Franklin, P. Swanson, W. Longstreth Jr, H. Checkoway, Pesticides and risk of Parkinson disease: a population-based case-control study, Archives of Neurology. 62 (2005) 91.

[50] A. Wang, S. Costello, M. Cockburn, X. Zhang, J. Bronstein, B. Ritz, Parkinson's disease risk from ambient exposure to pesticides, European Journal of Epidemiology. 26 (2011) 547–555.

[51] R. Harari, J. Julvez, K. Murata, D. Barr, D.C. Bellinger, F. Debes, et al., Neurobehavioral deficits and increased blood pressure in school-age children prenatally exposed to pesticides, Environmental Health Perspectives. 118 (2010) 890.

[52] P.G. Kopf, M.K. Walker, Overview of developmental heart defects by dioxins, PCBs, and pesticides, Journal of Environmental Science and Health, Part C. 27 (2009) 276–285.

[53] M.F. Bouchard, D.C. Bellinger, R.O. Wright, M.G. Weisskopf, Attention-deficit/hyperactivity disorder and urinary metabolites of organophosphate pesticides, Pediatrics. 125 (2010) e1270–e1277.

[54] M. Krstevska-Konstantinova, C. Charlier, M. Craen, M. Du Caju, C. Heinrichs, C. De Beaufort, et al., Sexual precocity after immigration from developing countries to Belgium: evidence of previous exposure to organochlorine pesticides, Human Reproduction. 16 (2001) 1020–1026.

[55] T. Galloway, R. Handy, Immunotoxicity of organophosphorous pesticides, Ecotoxicology. 12 (2003) 345–363.

[56] D. Medina, A. Prieto, G. Ettiene, I. Buscema, A. Abreu de V, Persistence of organophosphorus pesticide residues in Limon River waters, Bulletin of Environmental Contamination and Toxicology. 63 (1999) 39–44.

[57] A. Delle Site, Factors affecting sorption of organic compounds in natural sorbents, water systems and sorption coefficients for

selected pollutants. A review, Journal of Physical and Chemical Reference Data. 30 (2001) 187–439.

[58] J.L. Acero, F.J. Real, F. Javier Benitez, A. González, Oxidation of chlorfenvinphos in ultrapure and natural waters by ozonation and photochemical processes, Water Research. 42 (2008) 3198–3206.

[59] A. Bermúdez-Couso, D. Fernández-Calviño, M. Pateiro-Moure, J.C. Nóvoa-Muñoz, J. Simal-Gándara, M. Arias-Estévez, Adsorption and desorption kinetics of carbofuran in acid soils, Journal of Hazardous Materials. 190 (2011) 159–167.

[60] W.T. Tsai, C.W. Lai, K.J. Hsien, Effect of particle size of activated clay on the adsorption of paraquat from aqueous solution, Journal of Colloid and Interface Science. 263 (2003) 29–34.

[61] PAN, Paraquat, Pesticides News. (1996) 20–21.

[62] FAO, Paraquat dichloride - Food and Agriculture Organization of the United Nations - specifications and evaluations report, (2003).

[63] M. Brigante, P.C. Schulz, Adsorption of paraquat on mesoporous silica modified with titania: effects of pH, ionic

strength and temperature, Journal of Colloid and Interface Science. 363 (2011) 355–61.

[64] L.A. Summers, The bipyridinium herbicides, Academic Press Inc., 1980.

[65] M. Pateiro-Moure, C. Pérez-Novo, M. Arias-Estévez, R. Rial-Otero, J. Simal-Gándara, Effect of organic matter and iron oxides on quaternary herbicide sorption-desorption in vineyard-devoted soils, Journal of Colloid and Interface Science. 333 (2009) 431–438.

[66] CVRIA, Court of First Instance of the European Communities in Case T-229/04, Press release n.° 45/07, (2007).

[67] M. Watts, Paraquat, Pesticide Action Network Asia and the Pacific (2011).

[68] W. Amondham, P. Parkpian, C. Polprasert, R. Delaune, A. Jugsujinda, Paraquat adsorption, degradation, and remobilization in tropical soils of Thailand, Journal of Environmental Science and Health Part B. 41 (2006) 485–507.

[69] S.T. Hsu, T.C. Pan, Adsorption of paraquat using methacrylic acid-modified rice husk, Bioresource Technology. 98 (2007)

3617–3621.

[70] E. Union, Decision n^{o} 2455/2001/EC of the European Parliament and of the Council, Official Journal of the European Communities. (2001).

[71] S. Morais, O. Tavares, P. Paíga, C. Delerue-Matos, Determination of Chlorfenvinphos in Soils by Microwave-Assisted Extraction and Stripping Voltammetry with an Ultramicroelectrode, Analytical Letters. 40 (2007) 1085–1097.

[72] ATSDR, Toxicological Profile for Chlorfenvinphos, (1997).

[73] IUPAC, Chlorfenvinphos (Ref : OMS 166), IUPAC database, 2009.

[74] S. Türkoglu, Determination of genotoxic effects of chlorfenvinphos and fenbuconazole in *Allium cepa* root cells by mitotic activity, chromosome aberration, DNA content, and comet assay, Pesticide Biochemistry and Physiology. 103 (2012) 224-230.

[75] ATSDR, Public Health Statement for Chlorfenvinphos, (1997).

[76] J.S. Van Dyk, B. Pletschke, Review on the use of enzymes for the detection of organochlorine, organophosphate and carbamate

pesticides in the environment, Chemosphere. 82 (2011) 291–307.

[77] L. Getzin, Persistence and degradation of carbofuran in soil, Environmental Entomology. 2 (1973) 461–468.

[78] A. Tomasevic, G. Boskovic, D. Mijin, S. Djilas, E. Kis, The extremely high stability of carbofuran pesticide in acidic media, Acta Periodica Technologica. 190 (2007) 97–103.

[79] FMC, Furadan Facts, (http://www.furadanfacts.com), accessed at 12 of December of 2012.

[80] PAN-UK, Which Pesticides are Banned in Europe?, Food and Fairness Briefing. (2008).

[81] I.S. Kim, J.Y. Ryu, H.G. Hur, M.B. Gu, S.D. Kim, J.H. Shim, Sphingomonas sp. strain SB5 degrades carbofuran to a new metabolite by hydrolysis at the furanyl ring, Journal of Agricultural and Food Chemistry. 52 (2004) 2309–2314.

[82] M.T. Branch, Carbofuran: Risk characterization, California Environmental Protection Agency (2006).

[83] Q.-X. Yan, Q. Hong, P. Han, X.-J. Dong, Y.-J. Shen, S.-P. Li, Isolation and characterization of a carbofuran-degrading strain

Novosphingobium sp. FND-3, FEMS Microbiology Letters. 271 (2007) 207–13.

[84] G. Farahani, Z. Zakaria, A. Kuntom, D. Omar, B. Ismail, Adsorption and desorption of carbofuran in Malaysian soils, Advances in Environmental Biology. 1 (2007) 20–26.

[85] E. Tombacz, The role of reactive surface sites and complexation by humic acids in the interaction of clay mineral and iron oxide particles, Organic Geochemistry. 35 (2004) 257–267.

[86] H.H. Murray, Applied Clay Mineralogy: Occurrences, Processing and Applications of Kaolins, Bentonites, Palygorskitesepiolite, and Common Clays, Elsevier, 2006.

[87] J.H. Choy, S.J. Choi, J.M. Oh, T. Park, Clay minerals and layered double hydroxides for novel biological applications, Applied Clay Science. 36 (2007) 122–132.

[88] H. Murray, Applied clay mineralogy today and tomorrow, Clay Minerals. 34 (1999) 39–39.

[89] M. Koppelman, J. Dillard, A study of the adsorption of Ni (II) and Cu (II) by clay minerals, Clays and Clay Minerals. 25 (1977) 457–462.

[90] S. Goldberg, Effect of Saturating Cation, pH, and Aluminum and Iron Oxide on the Flocculation of Kaolinite and Montmorillonite, Clays and Clay Minerals. 35 (1987) 220–227.

[91] I. McKissock, E.L. Walker, R.J. Gilkes, D.J. Carter, The influence of clay type on reduction of water repellency by applied clays: a review of some West Australian work, Journal of Hydrology. 231-232 (2000) 323–332.

[92] H.H. Murray, Traditional and new applications for kaolin, smectite, and palygorskite: a general overview, Applied Clay Science. 17 (2000) 207–221.

[93] D. Penner, G. Lagaly, Influence of anions on the rheological properties of clay mineral dispersions, Applied Clay Science. 19 (2001) 131–142.

[94] L. Oliveira, Clay–iron oxide magnetic composites for the adsorption of contaminants in water, Applied Clay Science. 22 (2003) 169–177.

[95] D. Hradil, Clay and iron oxide pigments in the history of painting, Applied Clay Science. 22 (2003) 223–236.

[96] P. Aparicio, J. Perez-Bernal, E. Galan, M. Bello, Kaolin fractal dimension. Comparison with other properties, Clay Minerals. 39 (2004) 75–84.

[97] S. Patil, J. Zhang, K. Tawfiq, G. Chen, Role of Interfacial Interactions in the Deposition of Colloidal Clay Particles in Porous Media, Journal of Adhesion Science and Technology. 23 (2009) 1845–1859.

[98] M.O. Pereira, M.J. Vieira, L.F. Melo, The effect of clay particles on the efficacy of a biocide, Water Science and Technology. 41 (2000) 61–64.

[99] A. Meunier, Clays, Springer, 2005.

[100] B. Hameed, Equilibrium and kinetics studies of 2, 4, 6-trichlorophenol adsorption onto activated clay, Colloids and Surfaces A: Physicochemical and Engineering Aspects. 307 (2007) 45–52.

[101] C. Almeida, N. Debacher, A. Downs, L. Cottet, C. Mello, Removal of methylene blue from colored effluents by adsorption on montmorillonite clay, Journal of Colloid and Interface Science. 332 (2009) 46–53.

[102] Y. El Mouzdahir, A. Elmchaouri, R. Mahboub, A. Gil, S. Korili, Equilibrium modelling for the adsorption of methylene blue from aqueous solutions on activated clay minerals, Desalination. 250 (2010) 335–338.

[103] M. Auta, B. Hameed, Modified mesoporous clay adsorbent for adsorption isotherm and kinetics of methylene blue, Chemical Engineering Journal. 198 (2012) 219–227.

[104] N. Rauf, S. Tahir, J.-H. Kang, Y.-S. Chang, Equilibrium, thermodynamics and kinetics studies for the removal of alpha and beta endosulfan by adsorption onto bentonite clay, Chemical Engineering Journal. 192 (2012) 369–376.

[105] M. El Ouardi, S. Alahiane, S. Qourzal, A. Abaamrane, A. Assabbane, J. Douch, Removal of Carbaryl Pesticide from Aqueous Solution by Adsorption on Local Clay in Agadir, American Journal of Analytical Chemistry. 4 (2013) 72–79.

[106] E. Errais, J. Duplay, F. Darragi, I. M'Rabet, A. Aubert, F. Huber, et al., Efficient anionic dye adsorption on natural untreated clay: kinetic study and thermodynamic parameters, Desalination. 275 (2011) 74–81.

[107] WHO, Bentonite, kaolin, and selected clay minerals, World Health Organization - Environmental Health Criteria 231. (2005).

[108] S. Mustafa, S. Tasleem, A. Naeem, Surface charge properties of Fe_2O_3 in aqueous and alcoholic mixed solvents, Journal of Colloid and Interface Science. 275 (2004) 523–529.

[109] S.T. Hussain, Charge Characteristics of Oxides/Hidroxides in Aqueous and Organic Solvents, Peshawar University, PhD Thesis, 2001.

[110] R.M. Cornell, U. Schwertmann, The iron oxides: structure, properties, reactions, occurrences and uses, Wiley-VCH, 2003.

[111] B. Szalay, Iron oxide nanoparticles and their toxicological effects: in vivo and in vitro studies, Faculty of Medicine of University of Szeged, PhD Thesis, 2012.

[112] A.S. Madden, M.F. Hochella Jr, T.P. Luxton, Insights for size-dependent reactivity of hematite nanomineral surfaces through Cu^{+2} sorption, Geochimica Et Cosmochimica Acta. 70 (2006) 4095–4104.

[113] H. Guo, A.S. Barnard, Environmentally dependent stability of low-index hematite surfaces, Journal of Colloid and Interface Science. 386 (2012) 315-324.

[114] H.S. Kim, Y. Piao, S.H. Kang, T. Hyeon, Y.-E. Sung, Uniform hematite nanocapsules based on an anode material for lithium ion batteries, Electrochemistry Communications. 12 (2010) 382–385.

[115] J.S. Chen, T. Zhu, C.M. Li, X.W. Lou, Building Hematite Nanostructures by Oriented Attachment, Angewandte Chemie International Edition. 50 (2011) 650–653.

[116] K. Sivula, F. Le Formal, M. Grätzel, Solar Water Splitting: Progress Using Hematite (α-Fe_2O_3) Photoelectrodes, ChemSusChem. 4 (2011) 432–449.

[117] Y. Lin, G. Yuan, S. Sheehan, S. Zhou, D. Wang, Hematite-based solar water splitting: challenges and opportunities, Energy & Environmental Science. 4 (2011) 4862–4869.

[118] B.L. Lau, R. Huang, A.S. Madden, Electrostatic adsorption of hematite nanoparticles on self-assembled monolayer surfaces, Journal of Nanoparticle Research. 15 (2013) 1–10.

[119] P. Cai, X. He, A. Xue, H. Chen, Q. Huang, J. Yu, et al., Bioavailability of methyl parathion adsorbed on clay minerals and iron oxide, Journal of Hazardous Materials. 185 (2011) 1032–1036.

[120] J.L. Marco-Brown, C.M. Barbosa-Lema, R.M. Torres Sánchez, R.C. Mercader, M. dos Santos Afonso, Adsorption of picloram herbicide on iron oxide pillared montmorillonite, Applied Clay Science. 58 (2012) 25–33.

[121] A. Chevillard, H. Angellier-Coussy, S. Peyron, N. Gontard, E. Gastaldi, Investigating ethofumesate-clay interactions for pesticide controlled release, Soil Science Society of America Journal. 76 (2012) 420–431.

[122] S. Mehdi, M. Halimah, M. Nashriyah, B.S. Ismail, Adsorption and Desorption of Paraquat in Two Malaysian Agricultural Soils, American-Eurasian Journal of Sustainable Agriculture. 3 (2009) 555–560.

[123] A. Iglesias, R. López, D. Gondar, J. Antelo, S. Fiol, F. Arce, Adsorption of paraquat on goethite and humic acid-coated goethite, Journal of Hazardous Materials. 183 (2010) 664–668.

[124] D. Gondar, R. López, J. Antelo, S. Fiol, F. Arce, Adsorption of paraquat on soil organic matter: Effect of exchangeable cations and dissolved organic carbon, Journal of Hazardous Materials. 235-236 (2012) 218-223.

[125] S.-T. Hsu, W.-C. Lin, W.-F. Hsiao, C.-C. Lee, T.-C. Pan, T.-T. Wang, et al., Preparation of methacrylic acid-grafted chitin using

cerium (IV) ion and its application in adsorbing paraquat, Journal of Applied Polymer Science. 127 (2013) 760–764.

[126] E. González-Pradas, M. Villafranca-Sánchez, D. Rey-Bueno, M.D. Ureña-Amate, M. Fernández-Pérez, *et al.*, Removal of paraquat and atrazine from water by montmorillonite-(Ce or Zr) phosphate cross-linked compounds, Pest Management Science. 56 (2000) 565–570.

[127] Y. Seki, K. Yurdakoç, Paraquat adsorption onto clays and organoclays from aqueous solution, Journal of Colloid and Interface Science. 287 (2005) 1–5.

[128] D. Ait Sidhoum, M. Socías-Viciana, M. Ureña-Amate, A. Derdour, E. González-Pradas, N. Debbagh-Boutarbouch, Removal of paraquat from water by an Algerian bentonite, Applied Clay Science. 83-84 (2013) 441-448.

[129] W. Tsai, C. Lai, K. Hsien, The effects of pH and salinity on kinetics of paraquat sorption onto activated clay, Colloids and Surfaces A: Physicochemical and Engineering Aspects. 224 (2003) 99–105.

[130] J. Weber, S. Weed, Adsorption and desorption of diquat, paraquat, and prometone by montmorillonitic and kaolinitic

clay minerals, Soil Science Society of America Journal. 32 (1968) 485–487.

[131] M. Fernández-Pérez, M. Villafranca-Sánchez, F. Flores-Céspedes, F. Garrido-Herrera, S. Pérez-García, Use of bentonite and activated carbon in controlled release formulations of carbofuran, Journal of Agricultural and Food Chemistry. 53 (2005) 6697–6703.

[132] V.K. Gupta, I. Ali, V.K. Saini, others, Adsorption of 2, 4-D and carbofuran pesticides using fertilizer and steel industry wastes, Journal of Colloid and Interface Science. 299 (2006) 556–563.

[133] K. Rama Krishna, L. Philip, Adsorption and desorption characteristics of lindane, carbofuran and methyl parathion on various Indian soils, Journal of Hazardous Materials. 160 (2008) 559–67.

[134] R. Rojas, J. Morillo, J. Usero, L. Delgado-Moreno, J. Gan, Enhancing soil sorption capacity of an agricultural soil by addition of three different organic wastes, Science of The Total Environment. 458 (2013) 614–623.

[135] S. Navarro Garcia, M. Navarro, M. Camara, A. Barba, Cinétique d'adsorption du chlorfenvinphos et du méthidathion sur bentonite et kaolinite, Agronomie. 10 (1990) 473–477.

[136] M. Mear, J. Le Saint, M. Privat, Adsorption mechanisms of carbofuran on silica: structure, kinetics, and solubility influence., Ecotoxicology and Environmental Safety. 35 (1996) 163–73.

[137] J. Gao, J. Maguhn, P. Spitzauer, A. Kettrup, Sorption of pesticides in the sediment of the Teufelsweiher pond (Southern Germany). I: Equilibrium assessments, effect of organic carbon content and pH, Water Research. 32 (1998) 1662–1672.

[138] J. Rouquerol, F. Rouquerol, K.S.W. Sing, Adsorption by powders and porous solids, Academic Press, 1998.

[139] E.L. Cussler, Diffusion: Mass transfer in fluid systems, 3rd ed., Cambridge University Press, 1997.

[140] N. Sánchez-Jiménez, M. Sevilla, J. Cuevas, M. Rodríguez, J. Procopio, Interaction of organic contaminants with natural clay type geosorbents: Potential use as geologic barrier in urban landfill, Journal of Environmental Management. 95 (2012) S182–S187.

[141] M.C. Vagi, A.S. Petsas, M.N. Kostopoulou, T.D. Lekkas, Adsorption and desorption processes of the organophosphorus pesticides, dimethoate and fenthion, onto three Greek

agricultural soils, International Journal of Environmental Analytical Chemistry. 90 (2010) 369–389.

[142] V. Homem, A. Alves, L. Santos, Amoxicillin removal from aqueous matrices by sorption with almond shell ashes, International Journal of Environmental and Analytical Chemistry. 90 (2010) 1063–1084.

[143] W. Wang, W. Wang, X. Zhang, D. Wang, Adsorption of p-chlorophenol by biofilm components, Water Research. 36 (2002) 551–560.

[144] R.B. Garcia-Reyes, J.R. Rangel-Mendez, Adsorption kinetics of chromium (III) ions on agro-waste materials, Bioresource Technology. 101 (2010) 8099–8108.

[145] S. Azizian, Kinetic models of sorption: a theoretical analysis, Journal of Colloid and Interface Science. 276 (2004) 47–52.

[146] F.B. Aarden, Adsorption onto heterogeneous porous materials: equilibria and kinetics, Technische Universiteit Eindhoven, PhD thesis, 2001.

[147] I. Brás, Utilização de casca de pinheiro como adsorvente para remoção de pentaclorofenol de águas contaminadas, Faculdade

de Engenharia da Universidade do Porto, PhD thesis, 2005.

[148] P. Nkedi-Kizza, D. Shinde, M. Savabi, Y. Ouyang, L. Nieves, Sorption kinetics and equilibria of organic pesticides in carbonatic soils from South Florida, Journal of Environmental Quality. 35 (2006) 268–276.

[149] B.K. Nandi, A. Goswami, M.K. Purkait, Removal of cationic dyes from aqueous solutions by kaolin : Kinetic and equilibrium studies, Applied Clay Science. 42 (2009) 583–590.

[150] Y.S. Ho, Review of second-order models for adsorption systems, Journal of Hazardous Materials. 136 (2006) 681–689.

[151] X. Song, Y. Pan, W. Ma, Z. Cheng, *et al.*, Adsorption behaviour of crystal violet onto opal and reuse feasibility of opal-dye sludge for binding heavy metals from aqueous solutions, Chemical Engineering Journal. 193-194 (2012) 381-390.

[152] Y. Ho, G. Mckay, A comparison of chemisorption kinetic models applied to pollutant removal on various sorbents, Institution of Chemical Engineers. 76 (1998) 332–340.

[153] H. Qiu, L. Lv, B. Pan, Q. Zhang, W. Zhang, Q. Zhang, Critical review in adsorption kinetic models, Journal of Zhejiang University SCIENCE A. 10 (2009) 716–724.

[154] Y.S. Ho, G. McKay, Pseudo-second order model for sorption processes, Process Biochemistry. 34 (1999) 451–465.

[155] S.V. Jadhav, V.G. Pangarkar, Particle-liquid mass transfer in mechanically agitated contactors, Industrial & Engineering Chemistry Research. 30 (1991) 2496–2503.

[156] R. Viegas, M. Rodríguez, S. Luque, J. Alvarez, I. Coelhoso, J. Crespo, Mass transfer correlations in membrane extraction: analysis of Wilson-plot methodology, Journal of Membrane Science. 145 (1998) 129–142.

[157] S. Boon-Long, C. Laguerie, J. Couderc, Mass transfer from suspended solids to a liquid in agitated vessels, Chemical Engineering Science. 33 (1978) 813–819.

[158] O.S.G.P. Soares, J.J.M. Órfão, M.F.R. Pereira, Nitrate reduction catalyzed by Pd-Cu and Pt-Cu supported on different carbon materials, Catalysis Letters. 139 (2010) 97–104.

[159] F. Villacañas, M.F.R. Pereira, J.J.M. Órfão, J.L. Figueiredo, Adsorption of simple aromatic compounds on activated carbons, Journal of Colloid and Interface Science. 293 (2006) 128–136.

[160] H.F. Gorgulho, F. Gonçalves, M.F.R. Pereira, J.L. Figueiredo, Synthesis and characterization of nitrogen-doped carbon xerogels, Carbon. 47 (2009) 2032–2039.

[161] M.S.F. Santos, A. Alves, L.M. Madeira, Paraquat removal from water by oxidation with Fenton's reagent, Chemical Engineering Journal. (2011).

[162] J.S. Teodósio, M. Simões, M.A. Alves, L.F. Melo, F.J. Mergulhão, Setup and Validation of Flow Cell Systems for Biofouling Simulation in Industrial Settings, The Scientific World Journal. 2012 (2012).

[163] J. Teodósio, M. Simões, L. Melo, F. Mergulhão, Flow cell hydrodynamics and their effects on E. coli biofilm formation under different nutrient conditions and turbulent flow, Biofouling. 27 (2011) 1–11.

[164] A. Pereira, J. Mendes, L.F. Melo, Using nanovibrations to monitor biofouling, Biotechnology and Bioengineering. 99 (2008) 1407–1415.

[165] W.T. Tsai, C.W. Lai, K.J. Hsien, Adsorption kinetics of herbicide paraquat from aqueous solution onto activated bleaching earth, Chemosphere. 55 (2004) 829–37.

[166] C.S.F. Oliveira, Tratamento de águas contendo clorfenvinfos por oxidação com reagente de Fenton, Faculdade de Engenharia da Universidade do Porto, Master Thesis, 2010.

[167] T.L. Hsieh, M.M. Kao, Adsorption of carbofuran on lateritic soils, Journal of Hazardous Materials. 58 (1998) 275–284.

[168] D.R. Oliveira, Sujamento por partículas em suspensão aquosa - Interacções superficiais, Universidade do Minho, PhD Thesis, 1990.

[169] B. Nandi, A. Goswami, M. Purkait, Adsorption characteristics of brilliant green dye on kaolin, Journal of Hazardous Materials. 161 (2009) 387–395.

[170] C. Quintelas, H. Figueiredo, T. Tavares, The effect of clay treatment on remediation of diethylketone contaminated wastewater: Uptake, equilibrium and kinetic studies, Journal of Hazardous Materials. 186 (2011) 1241–1248.

[171] M. Sjöberg, L. Bergström, A. Larsson, E. Sjöström, The effect of polymer and surfactant adsorption on the colloidal stability and rheology of kaolin dispersions, Colloids and Surfaces A: Physicochemical and Engineering Aspects. 159 (1999) 197–208.

[172] T. Sen, S. Mahajan, K. Khilar, Adsorption of Cu^{2+} and Ni^{2+} on iron oxide and kaolin and its importance on Ni^{2+} transport in porous media, Colloids and Surfaces A: Physicochemical and Engineering Aspects. 211 (2002) 91–102.

[173] F. Bouzerara, A. Harabi, S. Achour, A. Larbot, Porous ceramic supports for membranes prepared from kaolin and doloma mixtures, Journal of the European Ceramic Society. 26 (2006) 1663–1671.

[174] K. Draoui, R. Denoyel, M. Chgoura, J. Rouquerol, Adsorption of paraquat on minerals: a thermodynamic study, Journal of Thermal Analysis and Calorimetry. 58 (1999) 597–606.

[175] A. de Keizer, Adsorption of paraquat ions on clay minerals. Electrophoresis of clay particles, Progress in Colloid & Polymer Science. (1990) 118–126.

[176] E. A. Smith, C.I. Mayfield, Effects of paraquat on selected microbial activities in soil, Microbial Ecology. 3 (1977) 333–343.

[177] M. Pateiro-Moure, A. Bermúdez-Couso, D. Fernández-Calviño, M. Arias-Estévez, R. Rial-Otero, J. Simal-Gándara, Paraquat and Diquat Sorption on Iron Oxide Coated Quartz Particles and the Effect of Phosphates, Journal of Chemical & Engineering Data. 55 (2010) 2668–2672.

[178] M. Ramos-Tejada, A. Ontiveros, J. Viota, J. Durán, Interfacial and rheological properties of humic acid/hematite suspensions, Journal of Colloid and Interface Science. 268 (2003) 85–95.

[179] N. Iordanova, M. Dupuis, K.M. Rosso, Charge transport in metal oxides: a theoretical study of hematite α-Fe_2O_3, The Journal of Chemical Physics. 122 (2005) 144305–144305.

[180] M.S. Santos, G. Schaule, A. Alves, L.M. Madeira, Adsorption of paraquat herbicide on deposits from drinking water networks, Chemical Engineering Journal. 229 (2013) 324-333.

[181] W.T. Tsai, K.J. Hsien, Y.M. Chang, C.C. Lo, Removal of herbicide paraquat from an aqueous solution by adsorption onto spent and treated diatomaceous earth, Bioresource Technology. 96 (2005) 657–63.

[182] J. Seader, E.J. Henley, D. Keith, Separation process principles, 2nd ed., John Wiley & Sons, Inc., 1998.

[183] G. Rytwo, D. Tropp, C. Serban, Adsorption of diquat, paraquat and methyl green on sepiolite: experimental results and model calculations, Applied Clay Science. 20 (2002) 273–282.

[184] W. Tsai, M. Hsieh, H. Sun, S. Chien, H. Chen, Adsorption of paraquat onto activated bleaching earth, Bulletin of Environmental Contamination and Toxicology. 69 (2002) 189–194.

[185] C. Giles, T. MacEwan, S. Nakhwa, D. Smith, A system of classification of solution adsorption isotherms, and its use in diagnosis of adsorption mechanisms and in measurement of specific surface areas of solids, Journal of the Chemical Society (Resumed). (1960) 3973–3993.

[186] R. Calvet, Adsorption of organic chemicals in soils, Environmental Health Perspectives. 83 (1989) 145–77.